ceramics

MDPI

Review

Manufacturing of Perovskite Solar Cells: Materials, Processing Strategies, and Pathways to Scalable Production

Lincoln Pinoski, Carter Stone, Alec Viloria, Bobbie VanSant, Chris Velasco and Pradeep L. Menezes *

Department of Mechanical Engineering, University of Nevada, Reno, NV 89557, USA
* Correspondence: pmenezes@unr.edu

Abstract

Perovskite solar cells (PSCs) have emerged as one of the most rapidly advancing photovoltaic technologies of the past decade, progressing from the initial demonstration of 3.8% power conversion efficiency (PCE) in 2009 to certified single-junction efficiencies exceeding 26% and perovskite–silicon tandem efficiencies exceeding 33.9% as of 2024. Their appeal resides in the combination of a broadly tunable bandgap achieved through compositional engineering of the ABX_3 perovskite crystal structure, compatibility with low-temperature solution processing, and the potential for manufacturing costs substantially below those of silicon photovoltaics. However, the translation of laboratory-scale performance to commercially viable modules at industrial throughput remains the central challenge in the field. This review provides a comprehensive and critically organized account of PSC manufacturing, spanning device architectures and material requirements, scalable deposition and coating technologies, charge transport layer integration and interface engineering, process control and crystallization strategies, post-treatment methods, artificial intelligence and machine learning-assisted manufacturing, module fabrication and encapsulation, advanced tandem and flexible device configurations, green chemistry and circular lifecycle strategies, and the critical barriers to commercialization. The review concludes with a strategic assessment of the technological, regulatory, and economic requirements for PSC technology to transition from pilot-scale demonstration to utility-scale deployment.

Keywords: perovskite solar cells; scalable manufacturing; tandem solar cells; lead-free perovskite; power conversion efficiency; crystallization

1. Introduction

The development of solar photovoltaic technology has been a continuous pursuit since the first practical solar cell was demonstrated by Chapin, Fuller, and Pearson at Bell Laboratories in 1954 [1]. Silicon remains the dominant photovoltaic material, with monocrystalline silicon cells achieving certified efficiencies of 26.95% in research configurations and commercial modules typically operating at 22–24% [2]. The silicon photovoltaic industry is a mature manufacturing ecosystem with established supply chains, well-characterized failure modes, and a levelized cost of electricity (LCOE) competitive with fossil fuel generation in many markets. Against this backdrop, the emergence of perovskite-structured photovoltaic materials, first demonstrated as a photovoltaic sensitizer by Kojima et al. in 2009 [1], represents one of the most significant developments in energy materials science of the past two decades, characterized by a rate of efficiency improvement without precedent in the history of photovoltaics.

Check for updates

Academic Editors: Gilbert Fantozzi and Vincent Garnier

Received: 7 July 2026
Revised: 3 August 2026
Accepted: 6 August 2026
Published: 9 August 2026

Copyright: © 2026 by the authors. Licensee MDPI, Basel, Switzerland. This article is an open access article distributed under the terms and conditions of the Creative Commons Attribution (CC BY) license.

Perovskite solar cells derive their name from the ABX_3 crystal structure first described for the mineral $CaTiO_3$ by Gustav Rose in 1839, and in the photovoltaic context, the structure most commonly comprises organic or inorganic cations (methylammonium, formamidinium, cesium) at the A-site, lead or tin at the B-site, and halide anions (iodide, bromide, chloride) at the X-site [3]. The direct bandgap and exceptionally high absorption coefficient of these materials enable high photon absorption in films just a few hundred nanometers thick (orders of magnitude thinner than silicon absorbers) with theoretical single-junction efficiency approaching 30.5% [3]. More significantly, compositional engineering of the A/B/X-site stoichiometry continuously tunes the bandgap across the range of approximately 1.1–2.3 eV, enabling both optimal single-junction performance and the design of tandem devices with spectral splitting capabilities that exceed the Shockley–Queisser single-junction limit [3,4].

Photovoltaic technologies include established crystalline-silicon modules, commercial thin-film systems such as CdTe and $Cu(In,Ga)Se_2$, and emerging platforms including organic, dye-sensitized, quantum-dot, and perovskite solar cells [5]. Crystalline silicon currently provides high efficiency, long service life, and a mature manufacturing infrastructure, but generally requires energy-intensive wafer production and relatively rigid module designs. Thin-film technologies reduce absorber thickness and can enable lightweight modules, although constraints related to material availability, toxicity, processing complexity, or efficiency may limit wider deployment. Organic and dye-sensitized devices offer low-temperature processing, flexibility, and tunable optical properties but continue to face lower efficiency and stability compared with mature inorganic photovoltaics. Metal oxides such as TiO_2, ZnO, Al_2O_3, SiO_2, CeO_2, Fe_2O_3, and WO_3 also play important roles in photovoltaic devices as photoactive materials, charge-transport layers, passivation coatings, optical layers, and environmental barriers [6,7]. Their properties, limitations, and application trends have recently been comparatively reviewed. Within this broader landscape, perovskite solar cells are particularly attractive because they combine strong optical absorption, tunable bandgaps, high power-conversion efficiency, low-temperature processing, and compatibility with flexible substrates and tandem architectures.

The manufacturing imperative for PSCs is clear. Unlike most photovoltaic materials that require high-temperature, energy-intensive processing (silicon crystal growth at >1400 °C; CIGS selenization above 500 °C), perovskite layers can be deposited from solution at temperatures below 150 °C on a wide variety of substrates, including flexible polymer films [8,9]. This compatibility with low-temperature processing and roll-to-roll manufacturing architectures creates the potential for per-watt manufacturing costs substantially below those of silicon, provided that the stability, reliability, and reproducibility requirements for commercial photovoltaic products can be satisfied. This review synthesizes the current state of PSC manufacturing knowledge across all dimensions necessary to evaluate this potential, from materials and device architecture through scalable deposition methods, interface engineering, AI-assisted manufacturing, module encapsulation, tandem integration, and commercialization pathways, and identifies the technical and regulatory gaps that must be resolved for PSC technology to achieve its commercial promise. Although recent reviews have individually examined scalable deposition, interface engineering, tandem architectures, artificial intelligence, stability, and commercialization, these topics are often treated as separate research areas. The distinctive perspective of this review is to evaluate them as interdependent components of perovskite solar-cell industrialization. Rather than focusing only on record efficiency or individual fabrication methods, this review examines how material selection, interface design, coating-window control, module-area scaling, operational stability, environmental safety, standardization, manufacturing yield, and techno-economic performance constrain one another.

While early PSC research was primarily driven by the pursuit of record power conversion efficiencies, the field has now entered a new stage in which the principal barriers to commercialization are based in manufacturability rather than performance. This review focuses not only on advances in materials and device performance, but also on the engineering, manufacturing, technoeconomic, and regulatory challenges that must be overcome for successful industrial deployment. By critically examining these aspects together, the review provides a comprehensive perspective on the transition of PSCs from laboratory-scale demonstrations to commercially viable photovoltaic technologies.

2. Manufacturing Requirements, Materials, and Device Architectures

2.1. Efficiency Benchmarks and Manufacturing Targets

The photovoltaic performance targets for PSCs must be evaluated against the established benchmarks of competing technologies. Monocrystalline silicon cells currently achieve certified research-cell efficiencies of 26.95%, while the highest certified PSC single-junction efficiency stands at approximately 26.7% as of 2024 [2,8]. However, a critical distinction exists between small-area research cells (typically < 1 cm^2) and the commercial module performance that determines real-world deployment viability. Silicon modules routinely achieve > 22% area-weighted efficiency, while the most advanced PSC modules at 100 cm^2 scale reach approximately 18–20% PCE, which is a gap that reflects the persistent challenges of maintaining film uniformity, minimizing defect density, and controlling crystallization across areas many orders of magnitude larger than laboratory test cells [8,10,11]. The highest projected single-junction theoretical efficiency for PSCs of approximately 30.5% is rooted in the material's direct bandgap, high absorption coefficient, and relatively long carrier diffusion lengths under optimized conditions [3]. Tandem architectures that pair PSC top cells with silicon or other perovskite bottom cells have broken the single-junction limit, with certified perovskite–silicon tandem efficiencies exceeding 33.9% as of 2024.

The application of PSCs in building-integrated photovoltaics (BIPV) illustrates the performance leverage available from high efficiency. Liu et al. demonstrated that a commercial building equipped with BIPV facades and solar windows in Sharjah, UAE, consumed 27.69% less electricity annually than an equivalent building without BIPV systems [12]. Translating such performance advantages into commercial reality requires PSC manufacturing processes that consistently deliver cells and modules meeting efficiency, stability, and reliability specifications at throughputs relevant to grid-scale deployment.

2.2. Materials: Absorber, Transport Layers, Electrodes, and Encapsulation

The multilayer architecture of a perovskite solar cell requires sequential deposition of materials with carefully matched energy levels, mechanical properties, and chemical compatibilities. Table 1 summarizes the principal functional layers of a PSC, their material options, functions, and key manufacturing challenges.

Table 1. Functional layers of a perovskite solar cell device architecture: principal material options, function in the device, and key manufacturing and stability challenges.

Component/Layer	Primary Materials	Function	Key Challenge	Reference
Perovskite absorber	$MAPbI_3$; $FAPbI_3$; mixed-cation/halide (Cs/FA/MA)(Pb/Sn)(I/Br)	Absorbs photons; generates electron-hole pairs; tunable bandgap 1.1–2.3 eV via A/B/X-site ion adjustment	Ion migration; phase instability; sensitivity to moisture, oxygen, UV; lead toxicity	[3,8,13,14]
Electron transport layer (ETL)	TiO_2 (anatase); SnO_2; ZnO; organic semiconductors (PCBM, C_{60})	Extracts electrons; blocks holes; transfers electrons to front electrode	Conduction band alignment; UV-induced degradation of TiO_2; high-temperature sintering requirement for dense TiO_2	[15–17]

Table 1. *Cont.*

Component/Layer	Primary Materials	Function	Key Challenge	Reference
Hole transport layer (HTL)	Spiro-OMeTAD (organic); PTAA; NiO_x (inorganic); P3HT; copper-based oxides	Extracts holes; blocks electrons; transfers holes to back electrode	High cost of spiro-OMeTAD; moisture sensitivity; dopant-induced degradation; energy-level alignment	[18–20]
Front electrode	FTO (fluorine-doped SnO_2); ITO; AZO; transparent conductive oxides	Collects carriers; transmits light; low sheet resistance	Sputtering damage to underlying layers; cost of ITO; mechanical brittleness on flexible substrates	[21–23]
Back electrode	Au; Ag; carbon; Cu	Collects majority carriers; forms ohmic contact	Gold cost; silver migration/corrosion; carbon electrode lower efficiency; solvent incompatibility during deposition	[24–26]
Encapsulant/barrier	Ethylene-vinyl acetate (EVA); UV-curable epoxy; TECP (thiol-ene photopolymer); polymer laminates	Seals device from moisture, O_2, mechanical damage; preserves long-term stability	Solvent release from EVA; adhesion to diverse layer chemistries; must not induce thermal stress	[26–28]
Substrate	Glass (borosilicate, soda-lime); PET; PEN; PI	Mechanical support; defines processing temperature window; must be optically transparent	Flexible polymer substrates restrict annealing temperature; glass mass limits portable applications	[8,9,23]

The perovskite absorber material presents the most complex materials engineering challenge in the device stack. Traditional lead-halide perovskites exhibit exceptional photovoltaic properties but suffer from chemical instability under exposure to moisture, oxygen, UV irradiation, and elevated temperatures, and from the mobility of halide ions within the crystal lattice, which drives phase segregation and electrochemical degradation under operational conditions [13,14]. The toxicity of lead (Pb) poses environmental and regulatory challenges for large-scale deployment, particularly regarding end-of-life waste management and potential leakage from damaged or degraded modules [29,30]. Improving the bandgap through increased cesium (Cs) or bromine (Br) content enhances thermal stability but introduces phase instability at intermediate compositions, requiring careful compositional optimization [21]. Lian et al. demonstrated that a supramolecular crown ether approach to passivating the perovskite grain boundaries reduced defect density and increased stability by constraining crystallization through host-guest chemistry [31]. The creation of mixed-cation mixed-halide perovskites has further enabled improved operating performance at low temperatures, with photoluminescence measurements confirming suppressed non-radiative recombination across the temperature range from 240 K to room temperature, providing evidence for the viability of PSC operation in cold climates and potentially in space applications [32].

2.3. Device Architectures: n-i-p, p-i-n, and Structural Variants

PSC device architectures are classified primarily by the sequence of charge-selective layers. The n-i-p (regular) configuration places the electron transport layer adjacent to the light-facing substrate, while the p-i-n (inverted) configuration positions the hole transport layer at the illuminated interface. Each architecture has distinct advantages and limitations relevant to manufacturing. Figure 1 shows a diagram of the differences between the regular and inverted stacks. The n-i-p architecture with TiO_2 as ETL is the configuration in which the highest certified efficiencies have been achieved, but TiO_2 requires high-temperature sintering (450–500 °C) incompatible with flexible polymer substrates and adds process complexity [15,16]. The p-i-n architecture offers lower processing temperatures (compatible with <150 °C substrates), better compatibility with self-assembled monolayer (SAM) HTLs, and generally superior performance in tandem configurations, and has achieved PCE values

exceeding 25% in recent optimized implementations [25]. The environmental sensitivity of PSC manufacturing environments is significant. Dust contamination disrupts crystal growth directionality and introduces grain boundary defects [33], while relative humidity must be maintained within approximately 30–40% for planar PSC fabrication, excess moisture causes Pb to migrate from the crystal framework, releasing iodine and inducing device collapse [34]. Manufacturing PSCs in cleanroom environments with controlled humidity is a fundamental process requirement. The tunable bandgap of the perovskite structure, adjustable through A/B/X-site compositional variation, is a key manufacturing advantage that enables device optimization for specific spectral conditions and tandem pairing requirements [3].

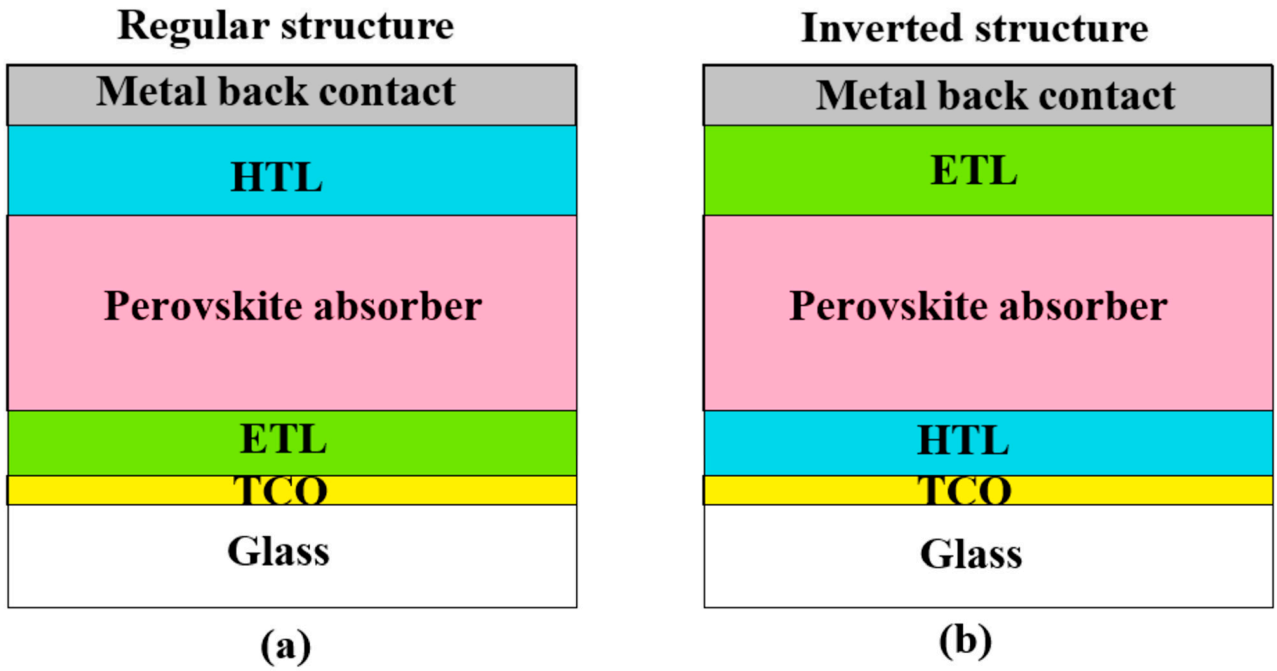


Figure 1. Diagram showing typical construction of PSC: (**a**) regular cell orientation; (**b**) inverted orientation. Reproduced from [35] Solar, 2025.

3. Scalable Deposition and Coating Technologies

3.1. From Laboratory to Industrial Scale: The Deposition Challenge

Scaling PSC production from the laboratory spin-coating process, which is optimal for small, precisely controlled areas but wastes 95–99% of the deposited solution, to industrial manufacturing processes capable of handling large substrates at high throughput represents the central manufacturing engineering challenge for PSC technology. The transition requires not only the substitution of scalable coating methods but the simultaneous optimization of ink formulations, crystallization control, drying parameters, and in-line quality monitoring to maintain the film quality achieved in laboratory conditions. Table 2 provides a systematic comparison of the principal deposition technologies in terms of scalability, film properties, material utilization, and roll-to-roll compatibility.

Table 2. Comparison of perovskite layer deposition technologies for scalable manufacturing: scalability, film properties, material utilization, roll-to-roll compatibility, and primary advantages and limitations.

Deposition Method	Scalability	Typical Film Thickness	Uniformity	Material Utilization	Roll-to-Roll Compatibility	Key Advantage	Primary Limitation	Reference
Spin coating	Lab only (batch)	50–500 nm	High (small area)	<5% (high waste)	No	Precise, reproducible; standard lab benchmark	Non-scalable; high material waste; substrate size limited to ~4 in	[10,36]
Spray coating	Medium-Large	50–1000 nm	Moderate	>80%	Possible	Non-contact; compatible with large-area; multi-layer capable	Sensitive to ambient conditions; requires parameter optimization; droplet uniformity critical	[36,37]
Blade/doctor-blade coating	Medium-Large	100–2000 nm	High (with control)	>90%	Yes	Scalable; precision thickness control; material efficient	Sensitive to humidity/temperature; requires crystallization control; ink formulation critical	[36,38]
Slot-die coating	Large (industrial)	50–500 nm	Very high	>95%	Yes (R2R standard)	Precision thickness; minimal waste; industrial standard for roll-to-roll	Requires optimized ink viscosity; drying and crystallization control critical	[24,36,39]
Vacuum/physical vapor deposition	Medium (batch)	50–500 nm	Very high	Moderate (<50%)	Limited	High-purity films; no solvent; precise thickness; ideal for inorganic layers	High equipment cost; difficult to co-deposit organic layers; not inherently R2R	[36,40]
Inkjet/printing	Medium-Large	100–2000 nm	Moderate-High	>90%	Possible	Digital patterning; material efficient; precise multi-layer deposition	Ink stability; nozzle clogging; printing speed vs. film quality trade-off	[36,38]

No single deposition technique is universally optimal for PSC manufacturing, as each presents distinct trade-offs between film quality, throughput, material utilization, process complexity, and manufacturing cost. Spin coating remains the preferred laboratory benchmark because of its film uniformity and reproducibility, but its high material waste and batch processing limit industrial relevance [41]. In contrast, blade coating and slot-die coating have emerged as the most promising scalable solution-processing methods due to their high material utilization, compatibility with continuous roll-to-roll manufacturing, and ability to produce uniform large-area films following appropriate optimization of ink rheology and crystallization conditions [42,43]. Spray coating offers advantages for non-contact deposition on large or irregular substrates but requires tighter control of droplet formation and ambient conditions, while inkjet printing provides digitally patterned deposition with excellent material efficiency but lower throughput. Vacuum deposition remains attractive where precise thickness control, solvent-free processing, and high-purity films are required, although its higher capital cost and reduced compatibility with continuous manufacturing currently limit widespread adoption for large-area absorber deposition [42]. Overall, current industrial development is increasingly centered on slot-die and blade coating, while hybrid manufacturing approaches combining multiple deposition techniques are expected to play an important role in future commercial PSC production.

3.2. Solution-Phase Coating Methods

Spray coating deposits perovskite precursor solutions as atomized aerosol droplets onto the substrate surface, and can be further developed into spray pyrolysis by applying the process to a heated substrate for simultaneous deposition and thermal decomposition of precursor components [36,37]. The technique is non-contact, compatible with large-area substrates, and can be configured for multi-layer deposition, making it suitable for scalable production of both the functional layers and the fluorine-doped tin oxide (FTO) electrode and semiconductor layers. Its sensitivity to ambient conditions, particularly temperature and humidity affecting droplet evaporation and film morphology, requires controlled deposition environments and careful parameter optimization to achieve film uniformity adequate for high-efficiency devices.

Beyond large-area coating, practical deployment also requires compatibility with established device-patterning and integration processes. Conventional photolithography is challenging for halide perovskites because water, polar solvents, photoresists, and processing chemicals can damage or dissolve the active material. Protective intermediate layers, such as parylene, can isolate the perovskite during processing and enable its integration with semiconductor fabrication methods. Such approaches may support scalable hybrid devices, although added barrier layers and processing steps must be optimized to avoid interfacial defects and performance losses [44].

Blade coating spreads a precursor solution across the substrate using a knife or blade element, with the film thickness controlled by the gap between the blade and substrate, the solution viscosity, and the relative velocity of blade and substrate. It can be integrated into roll-to-roll systems by mounting the blade assembly between an unwind and rewind roll, allowing continuous deposition followed by downstream drying and annealing stages [10,36]. Advances in blade coating for PSCs have included solvent engineering with dimethyl sulfoxide mixtures to control drying and nucleation, anti-solvent introduction during or after coating to promote rapid and uniform crystallization, and on-roll annealing to continuously treat freshly deposited films [45,46].

Slot-die coating delivers a precursor solution through a narrow precision die head onto the substrate in a controlled, uniform film whose thickness is determined by the flow rate, substrate speed, and die gap [36,39]. Its material utilization efficiency exceeds 95%, making

it the method of choice for cost-sensitive industrial applications, and it is the standard coating method for organic photovoltaic and perovskite module production lines [24]. Di Giacomo et al. demonstrated sheet-to-sheet PSC module production using slot-die coating on 6-inch substrates, achieving efficiencies competitive with spin-coated equivalents and establishing slot-die as the primary candidate for PSC industrial manufacturing [24]. The effectiveness of slot-die coating depends critically on solution viscosity and surface tension matching to the die geometry, drying condition control to prevent film defects during solvent evaporation, and precise mechanical calibration of the die gap for uniform film thickness across the full substrate width. Figure 2 shows a diagram of the typical slot-die coating process used for PSC manufacturing.

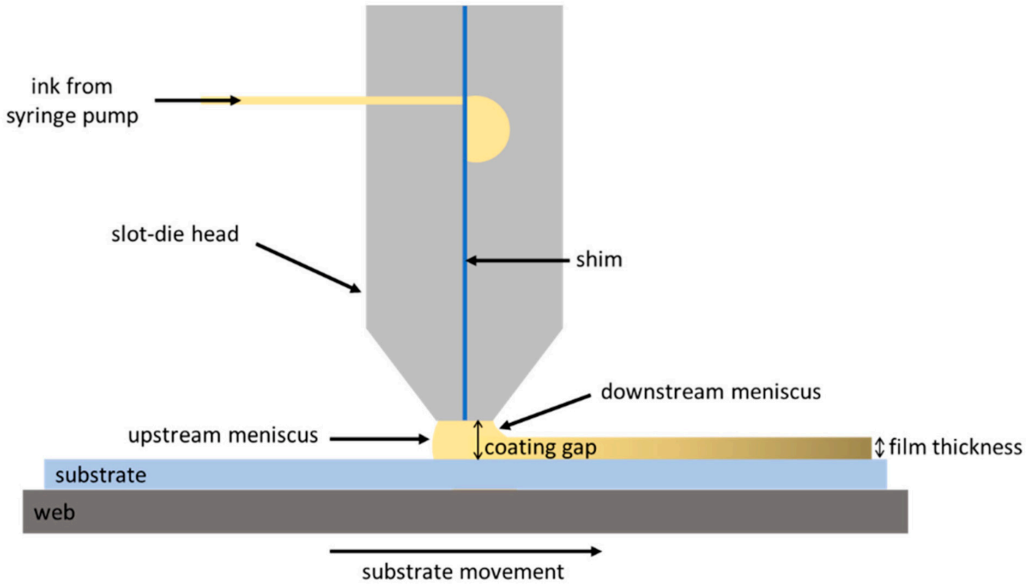


Figure 2. Diagram of slot-die coating system used for PSC processing. Reproduced from [47] Energies, 2024.

3.3. Vacuum Deposition Methods

Physical vapor deposition (PVD) methods, including thermal evaporation, co-evaporation, and sputtering, deposit perovskite constituent materials in a high-vacuum environment, condensing evaporated source materials onto the substrate as thin films [36,40]. The vacuum environment minimizes contamination, and the absence of solvents eliminates the crystallization and drying challenges that complicate solution processing. Co-evaporation of organic and inorganic components, simultaneously evaporating methylammonium iodide and lead iodide from separate sources at controlled rates to achieve the target perovskite stoichiometry on the substrate, simplifies the manufacturing process by combining layer synthesis and deposition into a single step. PVD processes are well-established in the semiconductor industry and provide excellent thickness and composition control, making them particularly suitable for the deposition of inorganic charge transport layers (TiO_2, SnO_2, NiO_x) where solution processing is less effective. Developments in PVD for PSC manufacturing include specialized equipment for flexible substrates, hybrid chemical vapor deposition approaches for mixed-cation and mixed-halide perovskite layers, and real-time thickness and composition monitoring systems [15,40].

3.4. Barriers to Industry Adoption

The dominant process variable limiting the coating window differs among deposition methods. For slot-die coating, the coating window is primarily governed by the relationship among ink flow rate, web speed, coating gap, and capillary number, which determines

meniscus stability and wet-film thickness [43]. At unsuitable operating conditions, defects such as air entrainment, bead breakup, ribbing, or edge instability can occur. For blade coating, the principal limiting variables are blade gap, coating speed, ink viscosity, and evaporation rate, because these parameters control shear, solution confinement, wet-film thickness, and crystallization during blade passage [43,48]. In gravure coating, cell geometry, ink transfer efficiency, and viscosity largely determine the deposited volume and pattern fidelity, while excessive web speed can reduce cell emptying and cause incomplete transfer. For spray-based coating, droplet size, solvent volatility, atomization pressure, and droplet coalescence define the usable process window, with insufficient coalescence producing rough or porous films and excessive wetting causing local flooding [43]. Accordingly, successful R2R manufacturing requires method-specific optimization of ink rheology, coating speed, wet-film thickness, drying rate, and substrate handling rather than direct translation of laboratory-scale coating parameters. These rheological constraints make the development of PSCs dynamic, requiring post-cured performance and ideal liquid properties for both manufacturable at-scale development and high efficiencies. The careful consideration required for effective manufacturing should sway research to include performance testing of manufacturing methods that can translate to large-scale production. Advancement in viable coatings using scalable methods would accelerate the adoption and therefore increase research of PSC technology.

4. Charge Transport Layer Integration and Interface Engineering

4.1. Transport Layer Functions and Material Requirements

The charge transport layers flanking the perovskite absorber perform two critical and opposing functions—selective extraction of one carrier type while blocking the other. The electron transport layer (ETL) extracts photogenerated electrons from the perovskite conduction band and transports them to the negative electrode, while blocking hole transport to prevent recombination at this interface. Conversely, the hole transport layer (HTL) selectively extracts holes and transports them to the positive electrode. The efficiency of these selective transport processes is characterized by low contact resistance, minimal energy barrier, and high carrier mobility and directly determines the device fill factor and open-circuit voltage. Interface engineering encompasses the set of manufacturing processes applied to the contact surfaces between the perovskite absorber and these transport layers to minimize energy barriers, trap states, and recombination centers that degrade device performance and stability [15,18]. Table 3 summarizes the principal interface engineering strategies with their mechanisms, targeted benefits, and representative material implementations.

Interfacial passivation improves PSC performance by reducing defect-mediated nonradiative recombination and optimizing interfacial energetics [49]. Undercoordinated Pb^{2+} ions, halide vacancies, and antisite defects create trap states that shorten carrier lifetime and reduce quasi-Fermi-level splitting, open-circuit voltage, and fill factor. Lewis acids or bases, ionic compounds, and molecular passivators can neutralize these defects, suppress vacancy formation, and lower trap-state density, thereby increasing carrier lifetime and voltage [50]. Self-assembled monolayers provide an additional benefit through interface dipoles that modify the local work function and improve energy-level alignment with the charge-transport layer, promoting selective carrier extraction while suppressing interfacial recombination [51,52]. However, excessive or electrically insulating passivation layers can impede charge transfer; therefore, effective interface engineering must balance chemical defect passivation, favorable energy-level alignment, and efficient carrier extraction. Mechanistic attribution should consequently combine photoluminescence, quasi-Fermi-level-splitting, impedance, transient, and trap-density measurements rather than relying solely on changes in device efficiency [53].

Table 3. Interface engineering strategies for perovskite solar cells: mechanism, primary benefit, representative materials or methods, and achieved performance improvements.

Strategy	Mechanism	Primary Benefit	Representative Materials/Methods	Achieved Improvement	Reference
Passivation of ETL/HTL interfaces	Ultrathin passivation layers fill surface defects, trap states, and recombination centers at perovskite/transport-layer interfaces	Reduces non-radiative recombination; improves VOC and fill factor	Phenethylammonium iodide (PEAI); organic ammonium halides; ionic liquids; small molecules	PCE improvements of 1–3% absolute; improved operational stability under thermal stress	[15,17,54]
Self-assembled monolayers (SAMs)	Bifunctional molecules anchor to substrate; functional head group tunes surface dipole and energy alignment	Precise energy level alignment without doping; improves hole selectivity in p-i-n architectures	MeO-2PACz; 2PACz; Me-4PACz; phosphonic acid anchors	p-i-n PCE >25%; enables low-temperature processed HTLs; improved stability	[18,25]
Energy level alignment tuning	Adjustment of CBM, VBM, and Fermi levels by material selection, doping, or compositional modification	Minimizes energy loss at interfaces; reduces VOC deficit; lowers charge recombination	Alkali metal doping of TiO_2/SnO_2; halide gradient at interfaces; oxide surface treatments	Voltage loss reduced to <0.3 V in optimized cells; improved carrier extraction efficiency	[16,55]
Inorganic HTL adoption	Replace organic spiro-OMeTAD with thermally stable inorganic HTLs	Improved moisture and thermal stability; lower dopant sensitivity; potentially lower cost	NiO_x (nanoparticle or sputtered); CuSCN; CuO_x	Improved T80 lifetime; suitable for low-temperature p-i-n processing on flexible substrates	[19,20,25]
Grain boundary passivation	Post-deposition treatment of grain boundaries with passivating agents	Reduces trap-state density; improves carrier lifetime; suppresses ion migration at boundaries	Alkali halide treatments; sulfur-containing ligands; Lewis acid/base pairs	Defect density reductions of 10–50%; notable PCE and stability improvements	[55–57]
Crystallization engineering	Solvent engineering, anti-solvent quenching, additive-controlled nucleation to tune grain size and morphology	Larger grains reduce grain boundary area; controlled morphology improves film uniformity	Dimethyl sulfoxide (DMSO) additive; anti-solvent (diethyl ether, chlorobenzene); $Pb(SCN)_2$ additive	Grain sizes increased from <500 nm to >1 µm; PCE and reproducibility improved	[45,46,56]

The interface engineering strategies summarized in Table 3 are complementary, with each addressing different loss mechanisms within PSCs. Passivation and grain-boundary treatments primarily suppress non-radiative recombination by reducing defect densities, whereas SAMs and energy-level tuning improve charge extraction through optimized band alignment [58]. Inorganic HTLs prioritize long-term thermal and moisture stability while reducing dependence on expensive organic materials, although they may require additional optimization to achieve equivalent charge transport performance [59]. Consequently, current high-efficiency devices increasingly combine multiple interface engineering strategies rather than relying on a single modification to simultaneously improve efficiency, stability, and manufacturability.

4.2. Energy Level Alignment and Passivation

Energy level alignment at the perovskite-transport layer interfaces is a prerequisite for efficient charge extraction and is quantified by the offset between the perovskite conduction band minimum (CBM) and the ETL CBM, and between the perovskite valence band maximum (VBM) and the HTL VBM. A small favorable offset (0.0–0.2 eV) promotes carrier extraction without introducing significant voltage loss, while a large offset or unfavorable alignment creates an energy barrier that impedes carrier transport and increases recombination losses [16]. Alignment is achieved through a combination of material selection, surface dipole engineering using self-assembled monolayers, and compositional doping of the transport layers to shift their Fermi levels into more favorable positions. SAMs such as MeO-2PACz and 2PACz deposited on ITO substrates as ultrathin hole-selective contacts have demonstrated particular effectiveness in p-i-n PSCs, providing precise energy alignment without the bulk doping requirements and associated instabilities of spiro-OMeTAD-based HTLs [18,25].

Passivation of interface trap states addresses the defect-driven recombination that is the primary efficiency-limiting mechanism at interfaces between the perovskite and transport layers. Surface defects arise from incomplete crystallization, halide vacancies, under-coordinated Pb atoms, and organic cation disorder at grain boundaries and film surfaces. Passivating agents, typically organic ammonium halides, zwitterionic molecules, or small organic molecules with Lewis base functional groups, coordinate with these undercoordinated sites, filling trap states and reducing non-radiative recombination [17,54]. Zhou et al. demonstrated that vertical interfacial engineering through dual-interface modification of two-step-processed perovskite films using NiO_x enabled high-efficiency p-i-n PSCs above 25% with improved operational stability [19], illustrating the impact of systematic interface engineering on both performance and reliability.

5. Process Control, Crystallization, and Post-Treatment

5.1. Process Control and Reproducibility

Reliable manufacturing of PSCs requires tight control of the environmental and process conditions governing crystallization, since perovskite film quality (grain size, defect density, morphology, and orientation) is highly sensitive to processing parameters. The supramolecular confinement approach developed by Liu et al. addresses this challenge by using crown ether host molecules to confine and guide perovskite crystal nucleation and growth, producing films with an average surface roughness below 10 nm and high electronic homogeneity that minimize batch-to-batch variation in power conversion efficiency [56]. This approach produces a highly reproducible fabrication outcome by replacing the stochastic, solvent-evaporation-driven crystallization of conventional spin coating with a controlled, host-guest-chemistry-guided nucleation process. Complementary process control improvements have been achieved through the incorporation of glutathione (GSH) as a redox

shuttle in tandem with its oxidized form glutathione disulfide (GSSG), which eliminates lead and tin oxidation impurities from the perovskite precursor solution before significant crystal growth has occurred [60]. By removing these redox-active impurities early in the crystallization process, GSH/GSSG treatment improves the consistency of the resulting perovskite film and reduces the occurrence of localized defects that would otherwise create performance-degrading recombination centers.

Although laboratory-scale PSCs have achieved remarkable power conversion efficiencies, these values are typically obtained using small-area devices fabricated under carefully controlled conditions that do not fully represent industrial manufacturing [61]. As device area increases, maintaining uniform film thickness, crystallization, composition, and interfacial quality becomes increasingly challenging, leading to greater performance variability, defect density, and efficiency losses. Furthermore, industrial viability depends not only on peak efficiency but also on statistical reproducibility, manufacturing yield, process robustness, and long-term operational stability across large-area modules [42]. Consequently, reported laboratory efficiencies should be interpreted alongside metrics such as active device area, batch-to-batch reproducibility, yield, and module performance to provide a more realistic assessment of commercial readiness.

5.2. Crystallization Engineering

Crystallization quality, encompassing grain size, grain boundary passivation, and defect density, is the primary determinant of perovskite absorber performance, as grain boundaries and lattice defects serve as non-radiative recombination centers that reduce carrier lifetime and device efficiency. Figure 3 shows a schematic of the typical crystal structure of a perovskite used in PSC. Sn-Pb mixed perovskite systems used in all-perovskite tandem bottom cells, tin oxidation (Sn^{2+} > Sn^{4+}) is a persistent crystallization problem that introduces deep-level trap states [62]. Yang et al. demonstrated that the introduction of sulfaguanidine (SG) into the perovskite precursor solution effectively suppresses tin oxidation through its strong binding to tin iodide species, delaying their release during crystallization and reducing defect formation, thereby improving both PCE and operational stability in Sn-Pb all-perovskite tandem solar cells [62]. Quantum dot (QD)-mediated crystallization offers an alternative strategy for controlling nucleation kinetics. QD films with matched crystal lattice parameters act as heterogeneous nucleation seeds that promote the growth of larger perovskite grains with reduced grain boundary area and density. Liu et al. showed that QD-mediated crystallization in two-step processed PSCs enhanced charge transport, reduced non-radiative recombination, and increased the PCE through both improved absorber quality and better charge extraction efficiency [57].

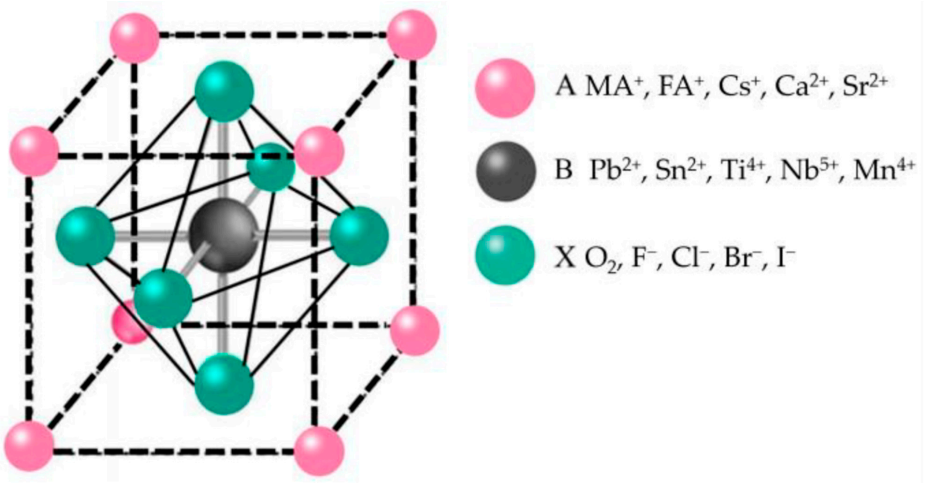


Figure 3. Typical crystal structure of a perovskite layer. Reproduced from [63], Coatings, 2023.

5.3. Post-Treatment Strategies

Post-deposition treatments extend the processing toolkit beyond crystallization control, enabling targeted remediation of specific defect types and interface quality improvements that cannot be achieved during the initial deposition step. Piperazinium chloride (PzCl) is a post-treatment agent whose small chloride anion radius facilitates downward migration through the perovskite film to the buried bottom interface, where chloride ions form passivating bonds with undercoordinated Pb sites and heal crystallographic defects without compromising carrier transport [64]. This selectivity for the bottom interface addresses a persistent challenge in wide-gap PSC fabrication, where many passivation strategies are effective for the top surface but less accessible for the buried interface. The improvement in PCE achieved by PzCl post-treatment has been attributed to simultaneous defect passivation and improved energy level alignment at the bottom contact. Nickel oxide (NiO_x) incorporation as a functional interface layer offers a different type of post-treatment benefit. When combined with the perovskite absorber, NiO_x provides thermally stable hole extraction, efficient charge carrier transport, and compatibility with low-temperature processing, with the combined effects of stability, efficiency, and cost contributing to an improved overall photovoltaic system [19].

6. Artificial Intelligence, Machine Learning, and Data-Driven Manufacturing

6.1. AI for Degradation Analysis and Performance Prediction

The complexity of PSC degradation, involving the simultaneous action of moisture, oxygen, UV photodegradation, ion migration, and thermal stress on multiple chemically diverse layers, creates a challenge for experimental characterization that is naturally suited to artificial intelligence analysis. Lee et al. reviewed the current state of data-driven and AI-integrated PSC research, documenting how machine learning has been applied across the full PSC development cycle from material discovery to self-driving laboratory implementation [65]. AI models trained on large datasets of PSC degradation behavior have demonstrated the ability to analyze complicated degradation pathways as functions of material composition and operating environment, generating predictions of performance trajectory and stability that would require years of sequential experimental testing to obtain by conventional means. These predictions enable rational design of both material compositions and encapsulation strategies targeted at the dominant degradation mechanisms rather than proceeding by empirical trial and error.

6.2. Machine Learning for Lead-Free Material Identification

One of the most impactful near-term applications of machine learning in PSC research is the accelerated identification of lead-free alternatives that retain the photovoltaic performance of lead-halide perovskites while eliminating the environmental and regulatory constraints associated with lead. Pabasara et al. applied an ensemble of machine learning models trained on computed material properties to screen a large compositional space of potential perovskite materials, identifying six candidates, namely $KBiBr_3$, $KZnBr_3$, $RbBiBr_3$, $RbZnBr_3$, $MAGeI_3$, and $FAGeI_3$, as viable lead-free alternatives based on predicted bandgap, stability, and carrier effective mass properties [66]. This ML-guided screening approach substantially compresses the material discovery timeline relative to exhaustive experimental synthesis and characterization, and the identified candidates provide concrete starting points for experimental validation. The elimination of lead would address the principal regulatory barrier to large-scale PSC deployment while simultaneously reducing the complexity of encapsulation and end-of-life management requirements.

6.3. Data-Driven Manufacturing and Large Language Models

Data-driven manufacturing extends the contribution of machine learning beyond material discovery into the optimization and control of PSC fabrication processes. Wang et al. [67] developed Perovskite-R1, which is a domain-specialized large language model (LLM) trained on thousands of perovskite-related scientific publications and designed specifically for the intelligent discovery of perovskite precursor additives and experimental design. The system demonstrated the ability to generate and rank candidate additives for improved stability and performance based on literature-derived structure-property relationships, substantially reducing the number of experiments needed to identify effective modifications. A complementary study by Liu et al. [68] applied five classical machine learning algorithms to 130 published datasets of PSC fabrication parameters and device performance, identifying over 100,000 parameter sets predicted to maximize device efficiency. The algorithms performed in approximately 10 min what would have required years of sequential experimental work, illustrating the transformative potential of data-driven approaches for manufacturing process optimization. Liu et al. additionally demonstrated that real-time machine learning parameter tuning of a flexible pressure-sensor fabrication process achieved performance levels unattainable through manual parameter adjustment, which is a precedent for closed-loop AI-controlled PSC manufacturing that is increasingly being implemented in pilot production lines.

For industrial PSC manufacturing, the most practical role of AI is not only material discovery but also real-time process monitoring and control. Data from in-line sensors, such as optical imaging, spectroscopy, thickness measurements, web tension, temperature, humidity, flow rate, and electrical testing, could be combined to detect defects, predict film quality, and adjust coating, drying, or annealing conditions during production. In a closed-loop system, the model would identify deviations from the desired process window and modify variables such as ink flow rate, web speed, coating gap, substrate temperature, or drying intensity before large quantities of defective material are produced [69,70].

Despite the growing use of artificial intelligence and machine learning in perovskite solar cell research, the scalability and generalizability of these approaches remain constrained by limited experimental data. Published datasets are often relatively small, fragmented across individual research groups, and generated using different material compositions, fabrication procedures, environmental conditions, device architectures, and characterization protocols [71]. In addition, inconsistent reporting of processing variables, stability-testing conditions, and measurement uncertainty makes it difficult to combine results from multiple studies into reliable training datasets. Models developed using narrowly defined or laboratory-specific data may therefore perform well within the original dataset but show limited transferability to other materials, processing systems, or manufacturing environments [72]. Progress will require standardized data formats, common terminology and metadata requirements, harmonized performance and degradation-testing protocols, and shared databases that include both successful and unsuccessful experiments. Greater adoption of FAIR data principles improves model reproducibility and enables more robust data-driven material discovery, degradation prediction, and process optimization.

7. Module Fabrication, Encapsulation, and Stability

7.1. Scaling from Cell to Module: Scribing, Interconnection, and Architecture

The transition from individual PSCs to interconnected modules introduces geometric and electrical integration requirements that reduce the module PCE below the single-cell value through two primary mechanisms, resistive interconnection losses and inactive (“dead”) area at cell boundaries. The monolithic module architecture, in which individual cells are defined by a series of three laser scribing steps (P1, P2, P3) that pattern successive layers, is the

standard approach for PSC module production, directly analogous to the scribing processes used for CIGS and CdTe thin-film modules [24,73]. Soto et al. demonstrated that nanosecond single laser patterning in an inverted PSC module architecture achieved a geometric fill factor of 99.3%, dramatically reducing the inactive area fraction relative to conventional multi-step scribing and thereby increasing the aperture-area module PCE [73]. The choice between n-i-p and p-i-n module architectures also has manufacturing implications. The p-i-n PSC modules can be processed at temperatures below 150 °C, enabling integration with flexible substrates and simplifying manufacturing line thermal management, while n-i-p architectures requiring high-temperature TiO_2 sintering add process complexity and restrict substrate options. Research by Dagar et al. demonstrated that compositional and interfacial engineering can enable p-i-n PSC mini-modules with high performance and stability, closing the historically observed efficiency gap between p-i-n and n-i-p configurations [25]. Current cell-to-module efficiency ratios for the best PSC modules approach 80–85%, compared to 95%+ for mature silicon modules, indicating significant headroom for improvement through interconnection loss reduction and yield enhancement. From a manufacturing perspective, monolithic laser-scribed interconnection is currently the most practical route for large-area PSC modules because it minimizes inactive area and is compatible with established thin-film production methods [74]. p-i-n device architecture modules offer advantages in low-temperature processing, flexible-substrate compatibility, and simplified thermal management, whereas n-i-p designs may retain benefits in material familiarity and laboratory-scale performance but often require higher processing temperatures. Future industrial development is therefore expected to increasingly favor p-i-n module architectures combined with high-precision laser scribing and improved process-yield control.

7.2. Encapsulation: Materials and Barrier Technologies

The long-term stability of PSC modules is fundamentally limited by the ingress of environmental stressors, primarily moisture and oxygen, through the encapsulation system, and the design of effective encapsulation is therefore a primary determinant of module lifetime under real operating conditions. Conventional encapsulation materials used in silicon modules, particularly ethylene-vinyl acetate (EVA) and polyolefin elastomers, are not optimal for PSCs because their curing and lamination processes release trace amounts of acetic acid that can degrade the perovskite layer and because their moisture vapor transmission rates, while adequate for silicon, may be insufficient for the more sensitive perovskite absorber [26,27]. Li et al. developed a solvent-free thiol-ene photopolymerized siloxane (TECP) encapsulant that addresses these limitations; the material polymerizes without solvent release, forms a dense, hydrophobic, mechanically robust network with high optical transparency and minimal thermal stress, and demonstrates complete polymerization without the residual monomer concerns associated with partial cure in conventional epoxy systems [27]. Critically, PCE measurements confirmed no degradation of the encapsulated device relative to the pre-encapsulation value, which is a result that has not always been achieved with solvent-based encapsulants. Barrier layer designs within the PSC stack provide an additional level of protection, with carbon and Mo-doped TiO_2 deployed to absorb harmful UV radiation and Al_2O_3 layers to suppress halide ion diffusion between layers, a migration pathway that contributes to interfacial degradation under operation [28]. Interfacial stability is also influenced by structural heterogeneity within charge-transport and barrier layers. Amorphous-crystalline interfaces can interrupt continuous diffusion pathways and improve barrier compactness, thereby limiting metal-electrode migration and corrosion. For example, engineered amorphous-crystalline ZrN_x barriers have been shown to suppress interfacial degradation in inverted perovskite solar cells, demonstrating that control of the barrier-layer microstructure can contribute significantly to long-term device stability [75]. The

need for structural and interfacial stabilization extends beyond photovoltaic modules to other halide-perovskite optoelectronic and photoelectrochemical systems. In these applications, exposure to illumination, electrolytes, electrical bias, and reactive species can accelerate defect formation, ion migration, phase decomposition, and interfacial corrosion. Passivation, protective charge-transport layers, and conformal encapsulation are therefore required to preserve both structural integrity and functional performance under application-specific operating conditions [76].

7.3. Reliability Testing: Accelerated Indoor and Outdoor Stability

The path to commercial PSC deployment requires demonstration of multi-decade operational stability under real-world conditions, which is a requirement that cannot be practically evaluated through real-time field testing alone, necessitating the development of accelerated aging protocols and validated methods for correlating accelerated laboratory results to expected field lifetimes. Jiang et al. developed an accelerated indoor stability testing approach for metal halide PSCs designed to correlate with six-month outdoor aging tests, applying individual stressors (illumination, temperature, humidity) at individually varied intensities to decouple their contributions to degradation rate [77]. Their results established that elevated temperature strongly accelerates PSC degradation under constant illumination, with stability degradation rate increasing nonlinearly as temperature rises, which is a finding directly relevant to module design for hot-climate deployment environments [77].

Establishing a rigorous framework for correlating accelerated laboratory results to field performance requires more than empirical trend identification. Chakar et al. applied drift-diffusion modeling combined with Bayesian statistical analysis to relate indoor accelerated test data to outdoor stability measurements through current density-voltage (JV) curve analysis [78]. The Bayesian framework treats each stressor as having a probability distribution of effects, runs multiple simulations with varied stressor combinations and intensities, and derives threshold values for each parameter that define the boundary between stable and degrading device behavior. This approach enables a mathematical comparison of indoor and outdoor test results without requiring identical test conditions, and accounts for the synergistic interactions between simultaneously acting stressors that are absent from single-stressor test protocols. Together, these complementary methodological contributions define the emerging framework for PSC stability qualification that will eventually need to be formalized into IEC standards analogous to those governing silicon module reliability testing.

Single stressor accelerated tests are useful for isolating individual degradation mechanisms, but they do not fully represent the coupled effects of illumination, humidity, temperature, and electrical bias experienced outdoors. Combined-stress testing supported by statistical and physical modeling offers a more realistic pathway for lifetime prediction, although it requires more complex equipment, larger datasets, and validated field correlations. Industrial qualification is therefore expected to move toward standardized combined-stress protocols aligned with IEC testing frameworks rather than relying solely on isolated laboratory aging experiments [79].

8. Advanced Manufacturing: Tandems, Flexible PV, and Sustainability

8.1. Tandem Device Integration and Manufacturing

Perovskite tandem solar cells exploit the tunable bandgap of the perovskite absorber to implement spectral splitting, in which different regions of the solar spectrum are absorbed and converted by optimally matched sub-cells, exceeding the Shockley–Queisser single-junction efficiency limit of approximately 33.5% for a single absorber material [4]. Table 4 compares the principal tandem architectures by junction configuration, certified efficiency, manufacturing compatibility, and key challenges.

Table 4. Comparison of perovskite tandem solar cell architectures: junction configuration, sub-cell materials, certified efficiency, manufacturing compatibility, and primary advantages and challenges.

Tandem Type	Junction Configuration	Top Cell Bandgap	Bottom Cell	Certified PCE (Record)	Manufacturing Compatibility	Primary Advantage	Key Challenge	Reference
Perovskite/silicon (2T monolithic)	Series-connected; shared recombination junction	~1.6–1.7 eV	c-Si (wafer-based)	~33.9% (2024)	High—builds on existing silicon lines; integration challenges at perovskite deposition step	Most commercially advanced; silicon infrastructure leveraged; highest PCE demonstrated	Thermal budget mismatch; perovskite deposition on textured silicon; long-term stability at interface	[4,80,81]
Perovskite/silicon (4T mechanically stacked)	Independent cells; optically coupled; separate electrodes	~1.6–1.8 eV	c-Si	~28–30%	Moderate—independent optimization of each cell; simpler interconnection	Independent optimization; no current matching required; existing silicon cell reuse	Lower practical PCE than 2T due to optical/electrical losses at interface; higher material cost	[4,22]
All-perovskite 2T tandem	Series-connected; tunable bandgap pair	~1.8 eV (wide-gap)	~1.2 eV (Sn-Pb narrow-gap)	~29.1% (2024)	All solution—processed; lightweight; flexible substrate compatible	Fully flexible possible; lower cost potential; all-perovskite processing synergy	Sn^{2+} oxidation instability; phase segregation in wide-gap cell; VOC deficit	[60,82,83]
Perovskite/CIGS	2T or 4T	~1.6–1.7 eV	CIGS thin film	~24–26%	Moderate—both thin-film; compatible processing temperatures	Lightweight; flexible substrate compatible; no silicon required	CIGS supply chain constraints; inter-layer compatibility; moisture sensitivity	[4,83]

The perovskite–silicon 2-terminal monolithic tandem is currently the most commercially advanced configuration, benefiting from the existing silicon photovoltaic manufacturing ecosystem and achieving the highest certified PCE of any tandem technology at over 33.9% [2,81]. Oxford PV has been the leading industrial developer of this technology, reporting pilot-line production of perovskite–silicon tandem modules with efficiencies substantially above any commercial single-junction module. The primary manufacturing challenge for 2T monolithic tandems is depositing the perovskite top cell on the textured surface of a standard silicon bottom cell, which presents significant coverage and uniformity challenges for solution-processed perovskite layers [80,81]. Sun et al. addressed an additional performance challenge in all-perovskite tandems by introducing a diammonium diiodide compound as an orientation-enhancing interlayer at the electron transport layer interface, which improved grain boundary filling, defect passivation, and fill factor in Sn-Pb binary bottom cells [82]. All-perovskite tandem designs benefit from the processability advantages of full solution processing and the potential for flexible module fabrication, but must contend with the instability of Sn-Pb narrow-gap bottom cells whose tin oxidation represents the most significant remaining performance limitation [83].

8.2. Flexible PSC Processing and Lightweight Applications

Flexible perovskite solar cells deposited on polymer substrates (PET, PEN, PI) enable lightweight, mechanically compliant photovoltaic systems for applications where rigid glass-substrate modules are impractical, such as building-integrated photovoltaics on curved architectural surfaces, portable power generation, wearable electronics, aerospace structures, and Internet-of-Things sensor platforms [8,9]. The processing of high-efficiency flexible PSCs requires all functional layers to be deposited at temperatures compatible with the substrate, generally below 150 °C, which restricts the choice of ETL materials away from high-temperature TiO_2 and toward low-temperature alternatives such as SnO_2 nanoparticles, ZnO, or C_{60}/PCBM [8,9]. Kim et al. demonstrated that flexible perovskite-crystalline silicon tandem cells combining the flexibility of polymer substrates with the efficiency of the silicon bottom cell represent a manufacturable pathway to high-performance flexible modules [9]. Chen et al. showed that semitransparent PSCs with transparent front electrodes achieve PCE sufficient for 23% efficiency four-terminal tandem configurations with high-efficiency silicon bottom cells [22]. Jafarzadeh et al. developed flexible, transparent, and bifacial PSCs using a wide-bandgap $FAPbBr_3$ absorber that enabled efficient conversion of both direct sunlight and diffuse indoor illumination, substantially expanding the deployment scenarios addressable by a single flexible PSC design [23].

8.3. Green Chemistry, Lead Management, and Circular Lifecycle Strategies

The environmental sustainability of PSC technology is conditioned by three interdependent factors, the toxicity of lead-containing absorber materials, the hazardous solvents required for solution processing, and the availability of viable end-of-life recycling pathways. Daskeviciute-Geguziene et al. demonstrated a green-chemistry-inspired synthesis of cyclobutane-based HTMs that mimic the spiro-type molecular configuration of the industry-standard spiro-OMeTAD without requiring the intensive synthesis conditions and hazardous reagents of the spiro synthesis route [20]. This approach reduces the environmental impact of HTM production while also improving the cost and scalability of the material, addressing the performance, economic, and sustainability dimensions of HTL manufacture. Green-solvent systems also involve important performance and processing tradeoffs. Conventional solvents such as *N*,*N*-dimethylformamide (DMF) and *N*-methyl-2-pyrrolidone (NMP) provide strong precursor solubility and favorable coordination with lead-halide complexes, enabling controlled nucleation and dense, uniform films, but present signifi-

cant toxicity and environmental concerns. Safer alternatives, including γ-butyrolactone, dimethyl sulfoxide-rich mixtures, acetonitrile, alcohol-based systems, and bio-derived solvents, may exhibit lower precursor solubility, different evaporation rates, or weaker intermediate-phase control [84]. These differences can narrow the coating window and promote incomplete coverage, pinholes, nonuniform crystallization, and greater sensitivity to humidity, coating speed, and drying conditions. Although green-solvent formulations have produced increasingly efficient devices, their reproducibility, large-area film quality, solvent recovery requirements, and compatibility with all functional layers remain less established than conventional solvent systems [85]. Future development should therefore prioritize solvent mixtures that simultaneously provide low toxicity, sufficient precursor dissolution, controllable drying kinetics, and compatibility with scalable coating methods.

Lead management strategies pursue two parallel approaches, physical containment through encapsulation and barrier layers, and chemical elimination through lead-free absorber development. Figure 4 shows a flow chart of recycling methods for PSCs, including the recoverable materials. Physical containment is implemented through polymer and inorganic barrier layers within the module stack that suppress ion migration and create physical separation between the Pb-containing perovskite layer and potential leakage pathways [26,29]. Lead-free alternatives using tin (Sn), bismuth (Bi), and cesium–titanium systems have been demonstrated computationally [30] and experimentally [66], with current efficiencies of 14–18%, lower than lead-halide perovskites but improving. Although lead-free perovskites offer a potentially safer route to PSC commercialization, their photovoltaic performance and operational stability remain substantially below those of lead-based systems. Tin-based perovskites are currently the most promising alternative because of their suitable band gaps and favorable carrier-transport properties. However, rapid oxidation of Sn^{2+} to Sn^{4+} causes self-doping, increased trap density, non-radiative recombination, and accelerated degradation in the presence of oxygen and moisture [86]. Yaoxu et al. reviewed PSC recycling technologies capable of recovering module materials at end of life through aqueous recycling (recovering entire modules with high material purity), layer-by-layer extraction (recovering high-value components individually), and detachable cell architectures (enabling cell-level recycling independent of the module assembly) [87]. Table 5 summarizes quantitative life cycle assessment metrics comparing PSC technology to incumbent photovoltaic technologies.

Encapsulation architecture strongly influences module integrity and lead leakage under extreme weather [88,89]. Rigid glass-glass or glass-back sheet modules provide high dimensional stability, low moisture permeability, and strong abrasion resistance, helping contain lead during normal operation. However, hail, debris, thermal shock, or heavy mechanical loads can fracture the glass and create rapid pathways for water ingress and lead release, particularly near damaged edges and perimeter seals [90]. Flexible modules replace glass with polymeric barrier films, reducing weight and brittle-fracture risk. However, repeated bending, impact, thermal mismatch, and outdoor aging may cause microcracking, puncture, delamination, and increased moisture permeation, producing gradual leakage pathways without obvious visible damage. Rigid modules may offer stronger environmental isolation but suffer severe localized leakage after fracture. Rigid designs require impact-resistant glass, durable edge seals, and internal lead-sequestering layers. Flexible designs additionally require high-barrier films, fatigue-resistant interfaces, mechanically tolerant components, and distributed lead-adsorbing materials. Standardized testing combining mechanical damage, moisture, ultraviolet exposure, thermal cycling, and hail or wind loading is needed to verify long-term containment [91].

Table 5. Life cycle assessment metrics comparing perovskite solar cell technology to silicon and CIGS photovoltaic technologies.

Metric	Single-Junction PSC	Perovskite–Silicon Tandem	Crystalline Silicon (Reference)	CIGS Thin-Film	Notes/Source	Reference
Energy payback time (EPBT)	~0.5–1.5 yr	~0.8–1.8 yr (combined)	~1.5–4 yr	~1–2 yr	Strongly dependent on manufacturing energy source and efficiency	[92]
CO_2 emissions (lifecycle)	~14–20 g CO_2-eq/kWh	~15–25 g CO_2-eq/kWh	~30–70 g CO_2-eq/kWh	~20–50 g CO_2-eq/kWh	Lower for PSC due to low-temperature processing and higher efficiency	[92]
Lead content (typical)	~0.5–1.0 g Pb/m^2	~0.4–0.8 g Pb/m^2 (PSC portion)	None	None	Comparable to Pb in solder in Si modules; manageable with encapsulation	[26,87]
Solvent/chemical waste	Moderate-High (DMF, DMSO)	Moderate (PSC layers)	Low	Low-Moderate	Green solvent (ethanol, 2-ME) substitution under development	[21,36,87]
End-of-life recyclability	Low (currently)	Low (currently)	Moderate (Si recycling mature)	Moderate	Aqueous/layer-by-layer recycling demonstrated at lab scale for PSC	[87]

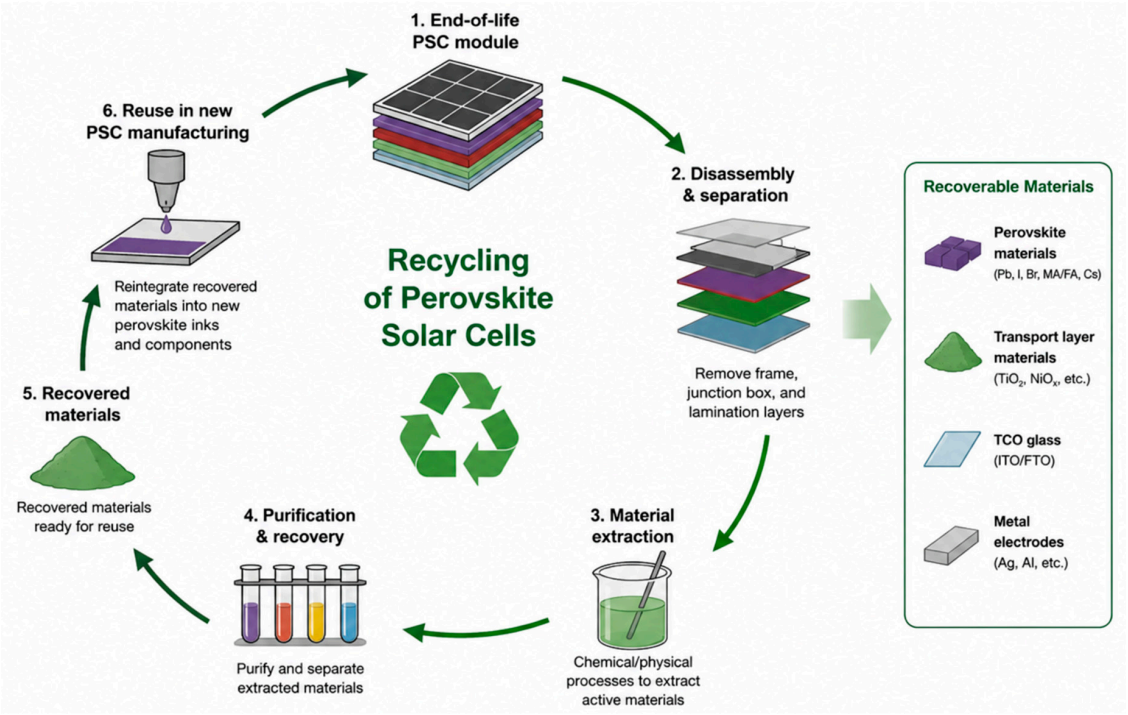


Figure 4. Recycling steps for the circular economy of PSCs.

9. Challenges and Pathways to Commercialization

The translation of PSC technology from research-level demonstrations to commercially viable, utility-scale manufacturing confronts a well-defined set of technical, economic, and regulatory barriers whose resolution will determine the pace and extent of market adoption. Table 6 provides a systematic analysis of the six principal challenge categories with their status and mitigation strategies.

Table 6. Systematic analysis of critical barriers to PSC commercialization: specific problem, current status, mitigation strategies, and progress to date.

Challenge Category	Specific Problem	Current Status	Mitigation Strategies	Progress to Date	Key References
Long-term stability	Ion migration; phase segregation; interface breakdown; sensitivity to moisture, O_2, UV, and thermal stress; intrinsic chemical instability of halide perovskites	T80 lifetime under ISOS-L-1 typically < 1000 h for unoptimized cells; best-in-class > 2000 h with encapsulation	Mixed-cation/halide perovskite compositions; 2D/3D heterostructures; inorganic HTLs (NiO_x); multifunctional encapsulation; compositional engineering with Rb/Cs additives	Encapsulated modules approaching 1000-h IEC stability tests; outdoor tests at Oxford PV > 1 yr	[13,14,93–95]
Scalable deposition uniformity	Non-uniform film formation, pinhole defects, and incomplete crystallization on large substrates; solvent evaporation and temperature gradients cause thickness variation at >100 cm^2	Efficiency drops from >25% (lab, ~0.1 cm^2) to ~18–20% (module, ~100 cm^2) are typical; gap narrowing with slot-die advances	Slot-die and blade coating with solvent engineering; in-line process monitoring; anti-solvent quenching adapted for R2R; machine learning-guided process control	Record 1 m^2 module PCE ~17–18%; slot-die reaching ~20% on 100 cm^2 substrates	[10,11,36,68,96]
Lead toxicity and environmental compliance	Pb-containing perovskites classified as hazardous; leakage risk during damage or end-of-life; regulatory barriers in several jurisdictions	Most high-efficiency PSCs (>23%) still use Pb; tin-based alternatives are 3–5% less efficient; EU RoHS exemptions under review	Physical barrier encapsulation (Al_2O_3, polymer layers); lead-sequestering materials in packaging; lead-free Sn, Ge, Bi alternatives; closed-loop recycling processes	Lead-free cells have reached ~16–17% PCE; ML identified 6 lead-free candidate materials; recycling demonstration at module scale	[29,30,66,87]
Technoeconomic and manufacturing cost	High capital investment for new equipment; solvent recovery costs; cleanroom humidity control; specialized chemicals with limited supply; current LCOE not competitive with mature silicon	Estimated LCOE ~5–8 US¢/kWh (projected at scale) vs. silicon ~3–4 US¢/kWh currently; upfront costs ~30–50% higher than silicon per MW	Lower-cost carbon electrodes; simplified processing (vacuum-free); co-processing with silicon lines for tandems; economy of scale through R2R volume	Oxford PV achieved first commercial tandem module sales 2023; NREL tracks improving cost trajectories	[81,96,97]

Table 6. *Cont.*

Challenge Category	Specific Problem	Current Status	Mitigation Strategies	Progress to Date	Key References
Standardized testing and certification	No PSC-specific IEC performance and durability standards; ISOS protocols used but not regulatory; comparison across studies difficult	IEC 61215 [98] (silicon standard) partially applied; ISOS-D/L/O protocols widely used in research but lack certification status	ISOS-defined protocol suite; drift-diffusion, Bayesian modeling for indoor-outdoor lifetime correlation; industry consortium (KACST, EPFL, Oxford PV) working on IEC PSC standard	IEC TC82 WG2 developing PSC-related standards; indoor-outdoor correlation validated for specific PSC stacks.	[77,78,94]
Process integration and supply chain	Adapting silicon manufacturing lines for perovskite; purity requirements for precursor chemicals; limited suppliers for high-purity MAI, FAI, and Cs salts; thermal expansion mismatch in tandem integration	Pilot lines at ~1 MW scale operational (Oxford PV, Saule Technologies, Microquanta); full GW-scale production not yet demonstrated	Dedicated perovskite deposition tools under development (e.g., Aixtron, ULVAC); standardized precursor specifications; modular R2R line architecture	Saule Technologies announced 100 MW/yr line (2024); Oxford PV pilot line operational for tandem	[2,81,96]

ISOS = International Summit on Organic Photovoltaic Stability; IEC = International Electrotechnical Commission; R2R = roll-to-roll; LCOE = levelized cost of electricity.

9.1. Long-Term Stability and Degradation Mechanisms

The stability deficit of PSCs relative to mature silicon modules is quantifiable. While commercial silicon modules carry 25-year performance warranties with less than 20% power degradation, the most stable PSC modules reported to date achieve approximately 1000–2000 h of operational lifetime under ISOS-L-1 illumination conditions before reaching the T80 threshold (80% of initial PCE) [13,93,94]. This represents a gap of approximately two orders of magnitude in operational lifetime that must be bridged before PSCs can satisfy the bankability requirements for commercial project financing. The fundamental causes of PSC degradation are multifactorial: moisture induces hydration and decomposition of the organic A-site cation; oxygen reacts with iodide vacancies to form reactive superoxide species that accelerate crystal lattice breakdown [99]; ion migration under electric field biasing or temperature gradients causes phase segregation in mixed-halide perovskites; and UV radiation photodegrades the TiO_2 ETL in n-i-p architectures, generating reactive oxygen species that attack the perovskite interface. Addressing these multiple, simultaneously active degradation mechanisms requires a systems approach. Compositional engineering (mixed-cation/halide formulations with Rb/Cs stabilizers) [95], inorganic HTL adoption (NiO_x replacing unstable spiro-OMeTAD) [19], 2D/3D heterostructure interfaces that limit ion migration [14], and robust multifunctional encapsulation [26,27] must all be implemented in concert rather than sequentially. The distinction between intrinsic material instability and extrinsic instability introduced by manufacturing impurities or interface defects is also critical. Process improvements that reduce defect density and improve interface passivation have been shown to substantially extend operational lifetime even without material substitution [100].

ISOS-L-1 and IEC qualification standards serve different purposes. ISOS-L-1 is primarily a research-oriented light-soaking protocol used to compare degradation behavior [79], whereas IEC standards apply defined stress conditions, test sequences, and pass-fail criteria at the module level [101]. A key limitation is that many current tests apply illumination, temperature, humidity, and electrical bias separately, even though perovskite modules may experience coupled degradation under simultaneous stress. Combined illumination, elevated temperature, and maximum-power-point operation can accelerate ion migration, interfacial reactions, phase instability, and local heating [102]. These combined-stress tests are especially difficult for large-area modules because irradiance and temperature must remain uniform across interconnected subcells while electrical bias is continuously controlled. Nonuniform illumination, thermal gradients, current mismatch, and local defects can produce hot spots and degradation modes that are not observed in small-area cells. Future

IEC-aligned protocols should therefore define requirements for combined stress exposure, irradiance and temperature uniformity, electrical-bias conditions, spatial monitoring, and degradation acceptance criteria.

9.2. Scalable Deposition and Yield at Industrial Scale

The efficiency gap between small-area research cells and large-area production modules is a quantitative measure of the manufacturing challenge. The world-record small-area PSC PCE of approximately 26.7% corresponds to a module efficiency on 100 cm^2 substrates of approximately 18–20%, representing a relative loss of 25–33% in going from cell to module scale [8,10,11]. This gap arises from multiple sources, such as edge effects and the dead area of scribing lines, the difficulty of maintaining film uniformity over large areas during solution coating and crystallization, and the statistical probability of performance-degrading defects increasing with module area. In commercial manufacturing, the control of film uniformity is more demanding than in research settings because small deviations in coating speed, solution temperature, ambient humidity, or drying airflow accumulate across large substrates and long production runs. Statistical process control (SPC) with in-line feedback adjustment of deposition parameters (monitored through optical profilometry, photoluminescence mapping, and four-probe resistance measurements) is essential for maintaining PSC production within acceptable tolerance limits [96]. Saki et al. reviewed the journey from lab-scale to large-scale solution-processed PSC production, identifying solvent evaporation dynamics and substrate temperature gradients as the dominant sources of film non-uniformity in scaled processes [11].

9.3. Technoeconomic Analysis and Supply Chain Development

Technoeconomic analysis (TEA) of PSC manufacturing reveals both the potential cost advantages over silicon and the additional costs that must be overcome before those advantages are realized [97]. The raw material cost of perovskite absorbers is genuinely lower than silicon, the precursor chemicals for a perovskite layer cost on the order of USD 0.01–0.05 per watt-peak versus approximately USD 0.10–0.20 per watt-peak for silicon wafers. This material cost advantage is partially or fully offset by the need for cleanroom-controlled manufacturing environments, specialized coating and drying equipment, solvent recovery systems, and the more frequent replacement of process equipment compared to the longer-lifetime silicon production toolset [96,97]. Beyond raw material costs, the economic viability of PSC manufacturing depends strongly on capital expenditure, equipment depreciation, production yield, and capacity utilization. Specialized coating, drying, encapsulation, laser-scribing, and solvent-recovery systems require substantial initial investment, and their depreciation must be distributed across the total module output produced during the equipment lifetime. Consequently, low production volumes or underutilized pilot lines can result in high manufacturing costs even when material consumption is low. Manufacturing yield is equally important because defects such as coating nonuniformity, pinholes, scribing damage, and encapsulation failure increase scrap rates and reduce the number of saleable modules produced from a given material and energy input [103]. High-capacity utilization lowers the cost per module by spreading fixed labor, facility, maintenance, and depreciation expenses over a larger annual output, whereas frequent downtime, slow process cycles, or unstable production conditions increase unit cost. Therefore, realistic technoeconomic assessments should include sensitivity analyses for equipment lifetime, annual utilization, line throughput, and production yield rather than assuming continuous operation and near-perfect manufacturing performance [104]. The supply chain for high-purity PSC precursor chemicals, particularly high-purity formamidinium iodide (FAI), methylammonium bromide (MABr), and cesium iodide, is not yet established at the scale

and purity specification consistency required for industrial production, and small lot-to-lot variations in precursor purity have been shown to affect film quality and device performance in ways that require tighter supply chain specifications than are currently standard for research-grade materials [55,96]. Lead-related regulatory compliance, particularly the management of lead-containing waste streams, the establishment of encapsulation and module design standards that meet the EU RoHS directive's requirements for hazardous substance management, and the development of end-of-life recycling certification, adds compliance costs that must be factored into commercial manufacturing economics [87,97]. However, lead-related regulations differ across major photovoltaic markets, creating uncertainty for PSC commercialization. In the European Union, photovoltaic panels intended for permanent installation are currently excluded from the scope of the RoHS Directive, whereas other covered electronic products remain subject to lead restrictions. China has adopted similar hazardous-substance regulations with increasing emphasis on conformity assessment and concentration limits, while the United States primarily regulates lead through hazardous-waste management and recycling requirements rather than product-level restrictions. Consequently, future changes in regional regulations may influence module design, certification, and market access [105].

Commercial deployment also requires standardized methods for evaluating lead leakage from damaged modules. Although IEC 61215 and IEC 61730 [106] assess module reliability and safety, they do not establish quantitative acceptance criteria for lead release following mechanical damage. Current studies employ various immersion and simulated rainfall tests, making direct comparison difficult. The development of harmonized leakage standards and recycling requirements would reduce regulatory uncertainty, improve bankability, and enable more reliable technoeconomic assessments of PSC technologies [89].

9.4. Standardization, Regulatory Frameworks, and Pilot Commercialization

The absence of PSC-specific international performance and durability standards represents a significant market entry barrier, as project financiers and grid operators require certification to recognized standards before underwriting large-scale photovoltaic installations [94]. Silicon PV modules are certified under IEC 61215 (performance) and IEC 61730 (safety), standards developed over decades of industry-academic collaboration that define qualification test sequences, environmental exposure conditions, and failure criteria. Equivalent IEC standards for PSC modules are currently under development within IEC TC82 WG2, with the ISOS protocol suite serving as the primary research-grade stability evaluation framework in the interim. The establishment of clear testing and certification pathways that provide investors and manufacturers with bankable evidence of PSC performance and reliability will be as important to commercial deployment as the technical improvements to efficiency and stability that continue to be demonstrated in research laboratories. At the pilot commercialization level, Oxford PV has achieved the most advanced status, with tandem perovskite–silicon modules entering commercial sales in 2023 from a pilot line at Brandenburg an der Havel, demonstrating that the manufacturing challenges are not insurmountable and providing the first commercial data point for PSC module performance under field conditions [81]. Saule Technologies and Microquanta Semiconductor have demonstrated pilot PSC production lines at 100 kW/yr to 1 MW/yr scale, providing additional evidence of manufacturing feasibility while highlighting the remaining gap to the GW-scale production required for material market impact. Figure 5 summarizes the major technological and commercial milestones that must be achieved to transition perovskite solar cells from laboratory-scale demonstrations to large-scale industrial deployment.



Figure 5. Roadmap illustrates the progressive industrialization of perovskite solar cells from laboratory-scale device development through scalable manufacturing, regulatory qualification, commercial production, and large-scale adoption.

Techno-economic assessments of perovskite photovoltaic modules are highly sensitive to the assumed operational lifetime because the levelized cost of electricity is distributed over the total energy generated during system operation. Although high power-conversion efficiency and low-temperature manufacturing can reduce module production costs, these advantages may be offset if the modules require frequent replacement [107]. Many reported perovskite devices currently demonstrate T80 stability on the order of approximately 1000–2000 h under laboratory or accelerated testing conditions, which remains substantially below the multi-decade service life expected from mature crystalline-silicon photovoltaic modules [108]. Extending module lifetime increases cumulative energy generation while distributing the initial module, installation, and balance-of-system costs over a greater electricity output. Conversely, a short service life increases the LCOE through reduced lifetime energy yield, additional module replacement costs, repeated installation labor, transportation, system downtime, and end-of-life management [109]. Therefore, LCOE projections that assume silicon-like operating lifetimes without experimentally supported degradation data may substantially underestimate the cost of perovskite electricity.

10. Future Directions

10.1. Self-Healing Materials and Advanced Compositional Engineering

The development of PSC compositions with intrinsic defect tolerance and self-healing character represents one of the most impactful research directions for addressing the stability challenge. Self-healing in the context of PSCs refers to the capacity of the material to recover from ion migration-induced disorder, vacancy accumulation, or light-induced phase segregation when the perturbing stimulus is removed or reversed, for example, the recovery of mixed-halide perovskite compositions from photo-induced segregation in the dark [1,93]. Achieving this property requires compositional strategies that raise the energetic barriers to halide demixing while maintaining optimal optoelectronic properties, which is a design challenge that molecular dynamics simulation and machine learning-assisted compositional optimization are increasingly being applied to address [65,110]. Rubidium cation incorporation into multi-cation perovskite formulations was shown by Saliba et al. to stabilize the crystal lattice and improve both PCE and operational stability by filling A-site vacancies and reducing ion migration pathways [95]. Exposure to controlled humidity concentrations has been shown to transiently improve PSC photovoltaic performance through modification of excited-state dynamics, though extended exposure leads to structural degradation, an observation that highlights the complexity of environmental interactions with the perovskite structure and the importance of effective encapsulation in decoupling beneficial from harmful environmental effects [111,112].

10.2. Computational Material Discovery and Digital Manufacturing

Computational tools (density functional theory (DFT) for electronic structure prediction, molecular dynamics for stability and ion migration modeling, and machine learning for high-throughput materials screening) are transforming the material discovery process for PSCs from empirical trial-and-error to rational design [65,110]. The practical impact of this transformation is already evident in the ML-guided identification of lead-free perovskite candidates [66] and the data-driven optimization of PSC fabrication processes that compressed years of experimental work into minutes of computation [68]. The extension of these approaches through digital twin manufacturing, virtual replicas of entire PSC production lines that enable process optimization and failure prediction without disrupting physical production, is an emerging direction that combines real-time data acquisition from production equipment with physical models of film formation, crystallization, and degradation [65]. For high-volume PSC manufacturing, digital twins would enable adaptive process control, predictive maintenance of coating equipment, and rapid identification of the root causes of yield losses, capabilities that are standard in mature semiconductor manufacturing but not yet implemented in PSC pilot lines. The integration of AI-controlled in-line quality monitoring (machine vision defect detection, real-time photoluminescence mapping, automated JV curve analysis) with data-driven process control creates a closed-loop manufacturing system capable of maintaining product quality while adapting to process drift, which is a capability that is essential for the consistency requirements of commercial photovoltaic module production.

10.3. Flexible, Tandem, and Niche Market Pathways

The market development pathway for PSC technology is likely to proceed through niche applications before addressing the utility-scale market, following the precedent established by other advanced photovoltaic technologies [113]. Building-integrated photovoltaics on non-standard architectural surfaces, portable and wearable energy systems, indoor photovoltaics for IoT sensors and electronic shelf labels, and aerospace applications for unmanned aerial vehicles and small satellites all represent markets where the unique properties of PSCs, such as lightweight, flexible form factor, high efficiency under diffuse illumination, low-temperature processing onto unconventional substrates, provide advantages over incumbent silicon technologies that justify the premium associated with an immature manufacturing technology [23,114]. As manufacturing volumes build through these niche markets, the learning curve effects that have driven silicon PV cost reduction by 99% since 1977 will begin to apply to PSC manufacturing, progressively reducing per-watt costs and expanding the addressable market. Perovskite–silicon tandem technology is the most direct path to utility-scale deployment, leveraging the massive installed base of silicon manufacturing infrastructure while delivering efficiencies that silicon alone cannot achieve, and the demonstration of commercial tandem modules by Oxford PV establishes the existence proof for this pathway [81]. Regulatory clarity, particularly the resolution of lead-related environmental regulations and the establishment of IEC certification standards, will be a critical enabler for large-scale investment in PSC manufacturing capacity, and proactive engagement by the research and industrial communities in standards development processes will determine the timeline of this regulatory enablement.

11. Conclusions

Perovskite solar cells have demonstrated extraordinary performance in laboratory conditions, with single-junction efficiencies exceeding 26.7% and tandem efficiencies exceeding 33.9%, establishing their theoretical and practical potential as a transformative photovoltaic technology. The remaining gap to commercial deployment is primarily a

manufacturing challenge rather than a materials science limitation. The efficiency values achievable in research cells can in principle be preserved in module-scale production provided that film uniformity, defect density, and crystallization quality are maintained across areas many orders of magnitude larger than current research cells. Scalable deposition technologies, particularly slot-die coating and blade coating for solution processing, and co-evaporation for inorganic layers, have demonstrated this scaling is achievable at efficiencies of 18–20% on 100 cm^2 substrates, with continued improvement expected as process engineering matures.

Long-term operational stability remains the most critical barrier to PSC commercialization. The simultaneous action of moisture, oxygen, UV radiation, thermal stress, and internal ion migration creates a complex, multi-pathway degradation landscape that requires a comprehensive materials and engineering response. Mixed-cation/halide compositional stabilization, inorganic transport layer adoption, systematic interface passivation, and robust multifunctional encapsulation must be implemented together rather than sequentially. The emergence of accelerated stability testing methodologies and the Bayesian statistical frameworks for correlating accelerated laboratory results to field performance represent the scientific foundation for establishing PSC reliability certification standards, which is an essential step for commercial project financing.

A central challenge emerging from these developments is the need to balance efficiency, stability, and scalability rather than optimize each independently. Many record-efficiency devices rely on tightly controlled deposition conditions, complex interfacial treatments, and material combinations that are difficult to reproduce over large areas or may introduce long-term instability. Conversely, scalable manufacturing routes often require wider processing windows, faster coating and drying, and simpler layer stacks, which can reduce peak efficiency but improve yield, reproducibility, and cost. Stability-enhancing measures, including multilayer encapsulation, inorganic transport layers, and extensive passivation, can further increase process complexity and capital requirements. Commercially viable PSC modules will therefore require a compromise in which modest reductions in laboratory-scale efficiency are accepted in exchange for improved operational lifetime, manufacturing yield, and process robustness. Hybrid manufacturing strategies, scalable passivation methods, and integrated process control are likely to provide the most practical route toward balancing these competing requirements.

The integration of artificial intelligence and machine learning across material discovery, process optimization, and manufacturing quality control is accelerating progress at each stage of PSC development. From ML-guided identification of lead-free alternatives and AI-driven process parameter optimization to large language model-assisted precursor additive discovery and digital twin manufacturing, computational tools are compressing the development timeline in ways that manual experimentation alone could not achieve. Together with continued investment from both public research funding and private venture capital, the coordinated progress of materials science, manufacturing engineering, regulatory standardization, and supply chain development creates a realistic pathway for perovskite solar cells to transition from a promising research technology to a commercially deployed component of global sustainable energy infrastructure.

The evidence reviewed indicates that the primary challenge facing PSC technology has shifted from efficiency to manufacturing efficacy. Although rapid efficiency improvements have established PSCs as one of the most promising emerging photovoltaic technologies, further commercial progress is now constrained less by peak laboratory performance than by stability, manufacturing consistency, large-area reproducibility, and industrial reliability. Further research should prioritize scalable processing, robust quality control,

standardized qualification procedures, and environmentally responsible manufacturing alongside continued improvements in device efficiency.

Funding: This research received no external funding.

Data Availability Statement: No new data were created or analyzed in this study. Data sharing is not applicable to this article.

Acknowledgments: During the preparation of this manuscript, the authors used GPT 5.6 for the purposes of creating original figures, specifically Figure 4. The authors have reviewed and edited the output and take full responsibility for the content of this publication.

Conflicts of Interest: The authors declare no conflict of interest.

References

1. Kojima, A.; Teshima, K.; Shirai, Y.; Miyasaka, T. Organometal Halide Perovskites as Visible-Light Sensitizers for Photovoltaic Cells. *J. Am. Chem. Soc.* **2009**, *131*, 6050–6051. [CrossRef] [PubMed]
2. Green, M.A.; Dunlop, E.D.; Hohl-Ebinger, J.; Yoshita, M.; Kopidakis, N.; Bothe, K.; Hinken, D.; Rauer, M.; Hao, X. Solar Cell Efficiency Tables (Version 60). *Prog. Photovolt. Res. Appl.* **2022**, *30*, 687–701. [CrossRef]
3. Ju, Z.; Lv, R.; Ansari, A.A.; Lin, J. Recent Advances in Additive Manufacturing for Solar Cell Based on Organic/Inorganic Hybrid Materials. *InfoMat* **2025**, *7*, e70017. [CrossRef]
4. Malevu, T.D. *Perovskite Solar Cells: From Materials Science to Device Engineering*; Nova Science Publishers: Hauppauge, NY, USA, 2023; ISBN 979-8-89113-130-9.
5. Pastuszak, J.; Węgierek, P. Photovoltaic Cell Generations and Current Research Directions for Their Development. *Materials* **2022**, *15*, 5542. [CrossRef] [PubMed]
6. Suchikova, Y.; Nazarovets, S.; Konuhova, M.; Popov, A.I. Binary Oxide Ceramics (TiO_2, ZnO, Al_2O_3, SiO_2, CeO_2, Fe_2O_3, and WO_3) for Solar Cell Applications: A Comparative and Bibliometric Analysis. *Ceramics* **2025**, *8*, 119. [CrossRef]
7. Zhu, K.; Chen, Y.; Wang, Y.; Feng, M.; Zhao, Y. Progress of Solution-Processed Metal Oxides as Charge Transport Layers towards Efficient and Stable Perovskite Solar Cells and Modules. *Mater. Today Nano* **2022**, *20*, 100252. [CrossRef]
8. Green, M.A.; Dunlop, E.D.; Yoshita, M.; Kopidakis, N.; Bothe, K.; Siefer, G.; Hinken, D.; Rauer, M.; Hohl-Ebinger, J.; Hao, X. Solar Cell Efficiency Tables (Version 64). *Prog. Photovolt. Res. Appl.* **2024**, *32*, 425–441. [CrossRef]
9. Kim, S.; Hoang, V.Q.; Bark, C.W. Silicon-Based Technologies for Flexible Photovoltaic (PV) Devices: From Basic Mechanism to Manufacturing Technologies. *Nanomaterials* **2021**, *11*, 2944. [CrossRef] [PubMed]
10. Fang, Y.; Sun, J.; Tan, Y.; Yang, G.; Chen, H.; Gu, M.; Feng, Y.; Yang, M.; Liu, H.; Fang, J.; et al. Scalable Solution Soaking Quenching Technique Unlocks Efficient and Durable Wide Bandgap Perovskite Solar Modules. *Nat. Commun.* **2026**, *17*, 2824. [CrossRef] [PubMed]
11. Saki, Z.; Byranvand, M.M.; Taghavinia, N.; Kedia, M.; Saliba, M. Solution-Processed Perovskite Thin-Films: The Journey from Lab- to Large-Scale Solar Cells. *Energy Environ. Sci.* **2021**, *14*, 5690–5722. [CrossRef]
12. Liu, T.; Almutairi, M.M.S.; Ma, J.; Stewart, A.; Xing, Z.; Liu, M.; Hou, B.; Cho, Y. Solution-Processed Thin Film Transparent Photovoltaics: Present Challenges and Future Development. *Nano-Micro Lett.* **2025**, *17*, 49. [CrossRef] [PubMed]
13. Tress, W. Perovskite Solar Cells on the Way to Their Radiative Efficiency Limit—Insights Into a Success Story of High Open-Circuit Voltage and Low Recombination. *Adv. Energy Mater.* **2017**, *7*, 1602358. [CrossRef]
14. Meng, L.; You, J.; Yang, Y. Addressing the Stability Issue of Perovskite Solar Cells for Commercial Applications. *Nat. Commun.* **2018**, *9*, 5265. [CrossRef] [PubMed]
15. Pan, H.; Shao, H.; Zhang, X.L.; Shen, Y.; Wang, M. Interface Engineering for High-Efficiency Perovskite Solar Cells. *J. Appl. Phys.* **2021**, *129*, 130904. [CrossRef]
16. Wang, S.; Sakurai, T.; Wen, W.; Qi, Y. Energy Level Alignment at Interfaces in Metal Halide Perovskite Solar Cells. *Adv. Mater. Interfaces* **2018**, *5*, 1800260. [CrossRef]
17. Le Corre, V.M.; Stolterfoht, M.; Perdigón Toro, L.; Feuerstein, M.; Wolff, C.; Gil-Escrig, L.; Bolink, H.J.; Neher, D.; Koster, L.J.A. Charge Transport Layers Limiting the Efficiency of Perovskite Solar Cells: How To Optimize Conductivity, Doping, and Thickness. *ACS Appl. Energy Mater.* **2019**, *2*, 6280–6287. [CrossRef]
18. Fu, W.; Soliman, A.I.A.; Zheng, Y.; Zhou, Y.; Zhang, Y.; Shan, S.; Chen, H. Self-Assembled Monolayers for Perovskite Solar Cells. *Rev. Mater. Res.* **2025**, *1*, 100017. [CrossRef]
19. Zhou, W.; Liu, H.; Li, H.; Zhang, W.; Li, H.; Zhou, X.; Chen, R.; Zhang, W.; Shi, T.; Abate, A.; et al. Vertical Interfacial Engineering in Two-Step-Processed Perovskite Films Enabled by Dual-Interface Modification for High-Efficiency p-i-n Solar Cells. *Nano-Micro Lett.* **2026**, *18*, 157. [CrossRef] [PubMed]

20. Daskeviciute-Geguziene, S.; Zhang, Y.; Rakstys, K.; Kreiza, G.; Khan, S.B.; Kanda, H.; Paek, S.; Daskeviciene, M.; Kamarauskas, E.; Jankauskas, V.; et al. Green-Chemistry-Inspired Synthesis of Cyclobutane-Based Hole-Selective Materials for Highly Efficient Perovskite Solar Cells and Modules. *Angew. Chem.* **2022**, *134*, e202113207. [CrossRef]
21. Lian, X.; Ma, Q.; Luo, M.; Min, H.; Fu, W.; Wan, L.; Zuo, X.; Wang, K.; Chen, Y.; Xu, C.; et al. Toward Sustainable Manufacturing of Highly Efficient and Stable Semi-Transparent Perovskite Solar Cells: The Critical Role of Green Solvent Properties. *Nano Energy* **2024**, *131*, 110250. [CrossRef]
22. Chen, B.; Bai, Y.; Yu, Z.; Li, T.; Zheng, X.; Dong, Q.; Shen, L.; Boccard, M.; Gruverman, A.; Holman, Z.; et al. Efficient Semitransparent Perovskite Solar Cells for 23.0%-Efficiency Perovskite/Silicon Four-Terminal Tandem Cells. *Adv. Energy Mater.* **2016**, *6*, 1601128. [CrossRef]
23. Jafarzadeh, F.; Castriotta, L.A.; Legrand, M.; Ory, D.; Cacovich, S.; Skafi, Z.; Barichello, J.; De Rossi, F.; Di Giacomo, F.; Di Carlo, A.; et al. Flexible, Transparent, and Bifacial Perovskite Solar Cells and Modules Using the Wide-Band Gap $FAPbBr_3$ Perovskite Absorber. *ACS Appl. Mater. Interfaces* **2024**, *16*, 17607–17616. [CrossRef] [PubMed]
24. Di Giacomo, F.; Shanmugam, S.; Fledderus, H.; Bruijnaers, B.J.; Verhees, W.J.H.; Dorenkamper, M.S.; Veenstra, S.C.; Qiu, W.; Gehlhaar, R.; Merckx, T.; et al. Up-Scalable Sheet-to-Sheet Production of High Efficiency Perovskite Module and Solar Cells on 6-in. Substrate Using Slot Die Coating. *Sol. Energy Mater. Sol. Cells* **2018**, *181*, 53–59. [CrossRef]
25. Dagar, J.; Fenske, M.; Al-Ashouri, A.; Schultz, C.; Li, B.; Köbler, H.; Munir, R.; Parmasivam, G.; Li, J.; Levine, I.; et al. Compositional and Interfacial Engineering Yield High-Performance and Stable p-i-n Perovskite Solar Cells and Mini-Modules. *ACS Appl. Mater. Interfaces* **2021**, *13*, 13022–13033. [CrossRef] [PubMed]
26. Ma, S.; Yuan, G.; Zhang, Y.; Yang, N.; Li, Y.; Chen, Q. Development of Encapsulation Strategies towards the Commercialization of Perovskite Solar Cells. *Energy Environ. Sci.* **2022**, *15*, 13–55. [CrossRef]
27. Li, S.; Li, Y.; Wang, L.; Luo, L.; Rong, Y.; Song, H.; Guo, J.; Guo, R.; Li, X. Solvent-Free Thiol-Ene Photopolymerization for Non-Destructive Encapsulation of Perovskite Solar Cells. *Adv. Funct. Mater.* **2026**, *36*, e19377. [CrossRef]
28. Zhang, S.; Liu, Z.; Zhang, W.; Jiang, Z.; Chen, W.; Chen, R.; Huang, Y.; Yang, Z.; Zhang, Y.; Han, L.; et al. Barrier Designs in Perovskite Solar Cells for Long-Term Stability. *Adv. Energy Mater.* **2020**, *10*, 2001610. [CrossRef]
29. Wu, T.; Qin, Z.; Wang, Y.; Wu, Y.; Chen, W.; Zhang, S.; Cai, M.; Dai, S.; Zhang, J.; Liu, J.; et al. The Main Progress of Perovskite Solar Cells in 2020–2021. *Nano-Micro Lett.* **2021**, *13*, 152. [CrossRef] [PubMed]
30. Chakraborty, K.; Choudhury, M.G.; Paul, S. Numerical Study of Cs2TiX6 (X = Br^-, I^-, F^- and Cl^-) Based Perovskite Solar Cell Using SCAPS-1D Device Simulation. *Sol. Energy* **2019**, *194*, 886–892. [CrossRef]
31. Lian, X.; Jin, M.; Dai, W.; Lv, Y.; Luo, M.; Hu, Y.; Wang, Z.; Li, H.; Xu, C.; Jiang, D.; et al. A Supramolecular Approach to Improve the Performance and Operational Stability of All-Perovskite Tandem Solar Cells. *Nat. Commun.* **2025**, *16*, 7173. [CrossRef] [PubMed]
32. Yuce-Cakir, H.; Chen, H.; Ogunniranye, I.; Thon, S.M.; Yan, Y.; Song, Z.; Hamadani, B.H. Comparison of Electroluminescence and Photoluminescence Imaging of Mixed-Cation Mixed-Halide Perovskite Solar Cells at Low Temperatures. *Adv. Opt. Mater.* **2026**, *14*, e03522. [CrossRef]
33. Lacey, K.; Parvazian, E.; Potts, S.-J.; Dunlop, T.; McGettrick, J.; Seunarine, K.; Jewell, E.; Davies, M.; Carnie, M.; Watson, T. Manufacturing Planar Perovskite Solar Cells in Dusty Environments. *Commun. Mater.* **2025**, *6*, 266. [CrossRef]
34. Ma, Y.; Luo, C.; Zhan, C.; Wang, K.; He, J.; Gao, P.; Bi, Z.; Ma, Y.; Zhao, Q. Crystallization-Activated Moisture Barrier for High-Tolerance Manufacturing of Perovskite Solar Cells. *Sci. Adv.* **2025**, *11*, eady5703. [CrossRef] [PubMed]
35. Axelevitch, A.; Lugassy, D. Assessing the Possibility to Enhance the Stability of Hybrid Perovskite Solar Cells: A Brief Review. *Solar* **2025**, *5*, 37. [CrossRef]
36. Kan, C.; Luo, C.; Hou, Y. Scalable Deposition and Drying Methods toward Large-Area Monolithic Perovskite/Silicon Tandem Solar Cells. *Energy Environ. Sci.* **2026**, *19*, 1101–1123. [CrossRef]
37. Hwang, K.; Jung, Y.; Heo, Y.; Scholes, F.H.; Watkins, S.E.; Subbiah, J.; Jones, D.J.; Kim, D.; Vak, D. Toward Large Scale Roll-to-Roll Production of Fully Printed Perovskite Solar Cells. *Adv. Mater.* **2015**, *27*, 1241–1247. [CrossRef] [PubMed]
38. Burschka, J.; Pellet, N.; Moon, S.-J.; Humphry-Baker, R.; Gao, P.; Nazeeruddin, M.K.; Grätzel, M. Sequential Deposition as a Route to High-Performance Perovskite-Sensitized Solar Cells. *Nature* **2013**, *499*, 316–319. [CrossRef] [PubMed]
39. Liu, Y.; Wu, Z.; Yin, L.; Zhang, Z.; Wu, X.; Wei, D.; Zhang, Q.; Cao, F. High-Temperature Air-Stable Solar Absorbing Coatings Based on the Cermet of $MoSi_2$ Embedded in SiO_2. *Sol. Energy Mater. Sol. Cells* **2019**, *200*, 109946. [CrossRef]
40. Li, H.; Liu, M.; Li, M.; Park, H.; Mathews, N.; Qi, Y.; Zhang, X.; Bolink, H.J.; Leo, K.; Graetzel, M.; et al. Applications of Vacuum Vapor Deposition for Perovskite Solar Cells: A Progress Review. *iEnergy* **2022**, *1*, 434–452. [CrossRef]
41. Rong, Y.; Ming, Y.; Ji, W.; Li, D.; Mei, A.; Hu, Y.; Han, H. Toward Industrial-Scale Production of Perovskite Solar Cells: Screen Printing, Slot-Die Coating, and Emerging Techniques. *J. Phys. Chem. Lett.* **2018**, *9*, 2707–2713. [CrossRef] [PubMed]
42. Li, Z.; Klein, T.R.; Kim, D.H.; Yang, M.; Berry, J.J.; Van Hest, M.F.A.M.; Zhu, K. Scalable Fabrication of Perovskite Solar Cells. *Nat. Rev. Mater.* **2018**, *3*, 18017. [CrossRef]

43. Shin Thant, K.K.; Seriwattanachai, C.; Jittham, T.; Thamangraksat, N.; Sakata, P.; Kanjanaboos, P. Comprehensive Review on Slot-Die-Based Perovskite Photovoltaics: Mechanisms, Materials, Methods, and Marketability. *Adv. Energy Mater.* **2025**, *15*, 2403088. [CrossRef]
44. Cheng, C.; Zhu, C.; Huang, B.; Zhang, H.; Zhang, H.; Chen, R.; Pei, W.; Chen, Q.; Chen, H. Processing Halide Perovskite Materials with Semiconductor Technology. *Adv. Mater. Technol.* **2019**, *4*, 1800729. [CrossRef]
45. Wu, R.; Wang, C.; Jiang, M.; Liu, C.; Liu, D.; Li, S.; Kong, Q.; He, W.; Zhan, C.; Zhang, F.; et al. Progress in Blade-Coating Method for Perovskite Solar Cells toward Commercialization. *J. Renew. Sustain. Energy* **2021**, *13*, 012701. [CrossRef]
46. Han, Y.; Liu, J.; Wang, P.; Ma, H.; Cai, R.; Wang, M.; Bian, J.; Shi, Y. Large-Area Perovskite Solar Modules Based on Uniformity Engineering of Perovskite Films: The Critical Role of Methyldiphenylphosphine Oxide Additive. *ACS Appl. Mater. Interfaces* **2024**, *16*, 39312–39320. [CrossRef] [PubMed]
47. Duarte, V.C.M.; Andrade, L. Recent Advancements on Slot-Die Coating of Perovskite Solar Cells: The Lab-to-Fab Optimisation Process. *Energies* **2024**, *17*, 3896. [CrossRef]
48. Patidar, R.; Burkitt, D.; Hooper, K.; Richards, D.; Watson, T. Slot-Die Coating of Perovskite Solar Cells: An Overview. *Mater. Today Commun.* **2020**, *22*, 100808. [CrossRef]
49. Sherkar, T.S.; Momblona, C.; Gil-Escrig, L.; Ávila, J.; Sessolo, M.; Bolink, H.J.; Koster, L.J.A. Recombination in Perovskite Solar Cells: Significance of Grain Boundaries, Interface Traps, and Defect Ions. *ACS Energy Lett.* **2017**, *2*, 1214–1222. [CrossRef] [PubMed]
50. Stolterfoht, M.; Grischek, M.; Caprioglio, P.; Wolff, C.M.; Gutierrez-Partida, E.; Peña-Camargo, F.; Rothhardt, D.; Zhang, S.; Raoufi, M.; Wolansky, J.; et al. How To Quantify the Efficiency Potential of Neat Perovskite Films: Perovskite Semiconductors with an Implied Efficiency Exceeding 28%. *Adv. Mater.* **2020**, *32*, 2000080. [CrossRef] [PubMed]
51. Caprioglio, P.; Stolterfoht, M.; Wolff, C.M.; Unold, T.; Rech, B.; Albrecht, S.; Neher, D. On the Relation between the Open-Circuit Voltage and Quasi-Fermi Level Splitting in Efficient Perovskite Solar Cells. *Adv. Energy Mater.* **2019**, *9*, 1901631. [CrossRef]
52. Al-Ashouri, A.; Magomedov, A.; Roß, M.; Jošt, M.; Talaikis, M.; Chistiakova, G.; Bertram, T.; Márquez, J.A.; Köhnen, E.; Kasparavičius, E.; et al. Conformal Monolayer Contacts with Lossless Interfaces for Perovskite Single Junction and Monolithic Tandem Solar Cells. *Energy Environ. Sci.* **2019**, *12*, 3356–3369. [CrossRef]
53. Zhang, S.; Ye, F.; Wang, X.; Chen, R.; Zhang, H.; Zhan, L.; Jiang, X.; Li, Y.; Ji, X.; Liu, S.; et al. Minimizing Buried Interfacial Defects for Efficient Inverted Perovskite Solar Cells. *Science* **2023**, *380*, 404–409. [CrossRef] [PubMed]
54. Zhuang, J.; Mao, P.; Luan, Y.; Yi, X.; Tu, Z.; Zhang, Y.; Yi, Y.; Wei, Y.; Chen, N.; Lin, T.; et al. Interfacial Passivation for Perovskite Solar Cells: The Effects of the Functional Group in Phenethylammonium Iodide. *ACS Energy Lett.* **2019**, *4*, 2913–2921. [CrossRef]
55. Jeong, M.; Choi, I.W.; Go, E.M.; Cho, Y.; Kim, M.; Lee, B.; Jeong, S.; Jo, Y.; Choi, H.W.; Lee, J.; et al. Stable Perovskite Solar Cells with Efficiency Exceeding 24.8% and 0.3-V Voltage Loss. *Science* **2020**, *369*, 1615–1620. [CrossRef] [PubMed]
56. Liu, X.; Xie, J.; Zhou, Z.; Lian, H.; Sui, X.; Li, Q.; Lin, M.; Liu, D.; Yuan, H.; Gao, F.; et al. Reproducible Fabrication of Perovskite Photovoltaics via Supramolecule Confinement Growth. *Nano-Micro Lett.* **2026**, *18*, 67. [CrossRef] [PubMed]
57. Liu, H.; Jin, G.; Wang, J.; Zhang, W.; Qing, L.; Zhang, Y.; Lu, Q.; Yue, P.; Zhang, G.; Wei, J.; et al. Quantum Dots Mediated Crystallization Enhancement in Two-Step Processed Perovskite Solar Cells. *Nano-Micro Lett.* **2025**, *17*, 169. [CrossRef] [PubMed]
58. Azam, M.; Du, T.; Wan, Z.; Zhao, H.; Zeng, H.; Wei, R.; Brabec, C.J.; Luo, J.; Jia, C. Dual Functionality of Charge Extraction and Interface Passivation by Self-Assembled Monolayers in Perovskite Solar Cells. *Energy Environ. Sci.* **2024**, *17*, 6974–7016. [CrossRef]
59. Zhu, R.; Guan, N.; Wang, D.; Bao, Y.; Wu, Z.; Song, L. Review of Defect Passivation for NiO_x-Based Inverted Perovskite Solar Cells. *ACS Appl. Energy Mater.* **2023**, *6*, 2098–2121. [CrossRef]
60. Meng, R.; Du, L.; Li, C.; Wan, Z.; Shi, J.; Zhang, Y.; Liu, W.; Zhi, C.; Jia, C.; Tan, L.; et al. Nature-Inspired Redox Shuttle with Regenerable Antioxidant for Efficient All-Perovskite Tandem Solar Cells. *Nano-Micro Lett.* **2026**, *18*, 165. [CrossRef] [PubMed]
61. Correa-Baena, J.-P.; Abate, A.; Saliba, M.; Tress, W.; Jesper Jacobsson, T.; Grätzel, M.; Hagfeldt, A. The Rapid Evolution of Highly Efficient Perovskite Solar Cells. *Energy Environ. Sci.* **2017**, *10*, 710–727. [CrossRef]
62. Yang, M.; Tian, R.; Sun, K.; Meng, Y.; Bai, Y.; Zhou, S.; Pan, H.; Gao, J.; Lu, X.; Wang, J.; et al. Achieving Efficient All-Perovskite Tandem Solar Cells through the Modulation of Crystallization in Sn-Pb Perovskite Solar Cells. *Sci. China Chem.* **2025**, *68*, 5016–5024. [CrossRef]
63. Chen, Y.; Zhang, M.; Li, F.; Yang, Z. Recent Progress in Perovskite Solar Cells: Status and Future. *Coatings* **2023**, *13*, 644. [CrossRef]
64. Li, X.; Ying, Z.; Li, S.; Chen, L.; Zhang, M.; Liu, L.; Guo, X.; Wu, J.; Sun, Y.; Xiao, C.; et al. Top-Down Dual-Interface Carrier Management for Highly Efficient and Stable Perovskite/Silicon Tandem Solar Cells. *Nano-Micro Lett.* **2025**, *17*, 141. [CrossRef] [PubMed]
65. Lee, J.; Noh, J.; Lee, H.; Lee, Y.; Im, J.; Seo, J. Recent Advances in Data-driven and Artificial Intelligence-integrated Perovskite Solar Cells: From Design to Self-driving Laboratories. *InfoMat* **2026**, *8*, e70124. [CrossRef]
66. Pabasara, W.G.A.; Wijerathne, H.A.H.M.; Karunarathne, M.G.M.M.; Sandaru, D.M.C.; Abeygunawardhana, P.K.W.; Sewvandi, G.A. Exploring Nontoxic Perovskite Materials for Perovskite Solar Cells Using Machine Learning. *Discov. Mater.* **2025**, *5*, 123. [CrossRef]

67. Wang, X.-D.; Chen, Z.-R.; Guo, P.-J.; Gao, Z.-F.; Mu, C.; Lu, Z.-Y. Perovskite-R1: A Domain-Specialized Large Language Model for Intelligent Discovery of Precursor Additives and Experimental Design. *Commun. Mater.* **2026**, *7*, 86. [CrossRef]
68. Liu, H.; Liu, K.; Zhang, B.; Chen, Z.; Yang, Y.; Sun, Q.; Ye, T.; Poudel, B.; Wang, K.; Wu, C. Data-Driven Design of Scalable Perovskite Film Fabrication via Machine Learning–Guided Processing. *Carbon Energy* **2026**, *8*, e70164. [CrossRef]
69. Laufer, F.; Götz, M.; Paetzold, U.W. Deep Learning for Augmented Process Monitoring of Scalable Perovskite Thin-Film Fabrication. *Energy Environ. Sci.* **2025**, *18*, 1767–1782. [CrossRef] [PubMed]
70. Maize, K.; Mi, Y.; Cakmak, M.; Shakouri, A. Real-Time Metrology for Roll-To-Roll and Advanced Inline Manufacturing: A Review. *Adv. Mater. Technol.* **2023**, *8*, 2200173. [CrossRef]
71. Liu, Y.; Tan, X.; Liang, J.; Han, H.; Xiang, P.; Yan, W. Machine Learning for Perovskite Solar Cells and Component Materials: Key Technologies and Prospects. *Adv. Funct. Mater.* **2023**, *33*, 2214271. [CrossRef]
72. Li, J.; Pradhan, B.; Gaur, S.; Thomas, J. Predictions and Strategies Learned from Machine Learning to Develop High-Performing Perovskite Solar Cells. *Adv. Energy Mater.* **2019**, *9*, 1901891. [CrossRef]
73. Soto, A.E.R.; Duarte, V.C.M.; Mendes, A.; Andrade, L. Inverted Perovskite Solar Modules with 99.3% Geometrical Fill Factor via Nanosecond Single Laser Patterning. *Commun. Eng.* **2025**, *4*, 198. [CrossRef] [PubMed]
74. Jeong, Y.; Kim, Y.; Lee, H.; Ko, S.; Ham, S.S.; Jung, H.R.; Choi, J.H.; Kim, W.M.; Jeong, J.; Yoon, S.; et al. Laser Scribing for Perovskite Solar Modules of Long-Term Stability. *Sol. RRL* **2024**, *8*, 2301040. [CrossRef]
75. Xiao, M.; Yuan, G.; Lu, Z.; Xia, J.; Li, D.; Chen, Y.; Zhang, Y.; Pei, F.; Chen, C.; Bai, Y.; et al. Engineering Amorphous–Crystallized Interface of ZrN_x Barriers for Stable Inverted Perovskite Solar Cells. *Adv. Mater.* **2023**, *35*, 2301684. [CrossRef] [PubMed]
76. Kim, Y.; Lee, E.; Lee, S. Enhancing Stability in Next-Generation Photoelectrodes Such as Organic Semiconductor and Halide Perovskite-Based Photoelectrodes for Various Applications: Recent Advanced Passivation and Encapsulation Methods. *Exploration* **2026**, *6*, 20240020. [CrossRef] [PubMed]
77. Jiang, Q.; Tirawat, R.; Kerner, R.A.; Gaulding, E.A.; Xian, Y.; Wang, X.; Newkirk, J.M.; Yan, Y.; Berry, J.J.; Zhu, K. Towards Linking Lab and Field Lifetimes of Perovskite Solar Cells. *Nature* **2023**, *623*, 313–318. [CrossRef] [PubMed]
78. Chakar, J.; Erdil, U.; Burgaud, A.; Remec, M.; Abate, A.; Ulbrich, C.; Schlatmann, R.; Bonnassieux, Y.; Khenkin, M.; Puel, J. Bridging Accelerated Indoor Aging and Outdoor Stability of Perovskite Solar Cells Using a Bayesian Modeling Framework. *Sol. RRL* **2025**, *9*, e202500716. [CrossRef]
79. Khenkin, M.V.; Katz, E.A.; Abate, A.; Bardizza, G.; Berry, J.J.; Brabec, C.; Brunetti, F.; Bulović, V.; Burlingame, Q.; Di Carlo, A.; et al. Consensus Statement for Stability Assessment and Reporting for Perovskite Photovoltaics Based on ISOS Procedures. *Nat. Energy* **2020**, *5*, 35–49. [CrossRef]
80. Belbachir, M.A.; Djennati, A.Z.; Kerai, S.; Khaouani, M.; Rouigueb, H. Simulation Validation and Performance Optimization of Tandem Perovskite/Silicon Solar Cells Based on Experimental Single-Junction Perovskite Solar Cell. *J. Electron. Mater.* **2025**, *54*, 8618–8627. [CrossRef]
81. Lin, R.; Wang, Y.; Lu, Q.; Tang, B.; Li, J.; Gao, H.; Gao, Y.; Li, H.; Ding, C.; Wen, J.; et al. All-Perovskite Tandem Solar Cells with 3D/3D Bilayer Perovskite Heterojunction. *Nature* **2023**, *620*, 994–1000. [CrossRef] [PubMed]
82. Sun, R.; Wang, P.; Wang, T.; Zhang, L.; Ge, Z.; Qiao, L.; Ye, T.; Li, F.; Liu, W.; Wen, Y.; et al. An Orientation-Enhanced Interlayer Enables Efficient Sn–Pb Binary Perovskite Solar Cells and All-Perovskite Tandem Solar Cells with High Fill Factors. *Nano Lett.* **2025**, *25*, 138–146. [CrossRef] [PubMed]
83. He, R.; Ren, S.; Chen, C.; Yi, Z.; Luo, Y.; Lai, H.; Wang, W.; Zeng, G.; Hao, X.; Wang, Y.; et al. Wide-Bandgap Organic–Inorganic Hybrid and All-Inorganic Perovskite Solar Cells and Their Application in All-Perovskite Tandem Solar Cells. *Energy Environ. Sci.* **2021**, *14*, 5723–5759. [CrossRef]
84. Kim, B.J.; Choi, H.; Park, S.; Johansson, M.B.; Boschloo, G.; Kim, M. Eco-Friendly All-Layer Green Solvent Efficient Perovskite Solar Cells. *ACS Sustain. Chem. Eng.* **2024**, *12*, 13371–13381. [CrossRef]
85. Wilk, B.; Öz, S.; Radicchi, E.; Ünlü, F.; Ahmad, T.; Herman, A.P.; Nunzi, F.; Mathur, S.; Kudrawiec, R.; Wojciechowski, K. Green Solvent-Based Perovskite Precursor Development for Ink-Jet Printed Flexible Solar Cells. *ACS Sustain. Chem. Eng.* **2021**, *9*, 3920–3930. [CrossRef]
86. Lanzetta, L.; Webb, T.; Zibouche, N.; Liang, X.; Ding, D.; Min, G.; Westbrook, R.J.E.; Gaggio, B.; Macdonald, T.J.; Islam, M.S.; et al. Degradation Mechanism of Hybrid Tin-Based Perovskite Solar Cells and the Critical Role of Tin (IV) Iodide. *Nat. Commun.* **2021**, *12*, 2853. [CrossRef] [PubMed]
87. Gao, Y.; Jumayi, B.; Wei, P.; Song, C.; Wang, S.; Shen, X. From Waste to Value: A Comprehensive Review of Perovskite Solar Cell Recycling Technologies. *Crystals* **2025**, *16*, 24. [CrossRef]
88. Wang, Y.; Ahmad, I.; Leung, T.; Lin, J.; Chen, W.; Liu, F.; Ng, A.M.C.; Zhang, Y.; Djurišić, A.B. Encapsulation and Stability Testing of Perovskite Solar Cells for Real Life Applications. *ACS Mater. Au* **2022**, *2*, 215–236. [CrossRef] [PubMed]
89. Jiang, Y.; Qiu, L.; Juarez-Perez, E.J.; Ono, L.K.; Hu, Z.; Liu, Z.; Wu, Z.; Meng, L.; Wang, Q.; Qi, Y. Reduction of Lead Leakage from Damaged Lead Halide Perovskite Solar Modules Using Self-Healing Polymer-Based Encapsulation. *Nat. Energy* **2019**, *4*, 585–593. [CrossRef]

90. Sutherland, L.J.; Weerasinghe, H.C.; Simon, G.P. A Review on Emerging Barrier Materials and Encapsulation Strategies for Flexible Perovskite and Organic Photovoltaics. *Adv. Energy Mater.* **2021**, *11*, 2101383. [CrossRef]
91. Wu, P.; Wang, S.; Li, X.; Zhang, F. Beyond Efficiency Fever: Preventing Lead Leakage for Perovskite Solar Cells. *Matter* **2022**, *5*, 1137–1161. [CrossRef]
92. Gong, J.; Darling, S.B.; You, F. Perovskite Photovoltaics: Life-Cycle Assessment of Energy and Environmental Impacts. *Energy Environ. Sci.* **2015**, *8*, 1953–1968. [CrossRef]
93. Rolston, N.; Sleugh, A.; Chen, J.P.; Zhao, O.; Colburn, T.W.; Flick, A.C.; Dauskardt, R.H. Perspectives of Open-Air Processing to Enable Perovskite Solar Cell Manufacturing. *Front. Energy Res.* **2021**, *9*, 684082. [CrossRef]
94. Snaith, H.J. Present Status and Future Prospects of Perovskite Photovoltaics. *Nat. Mater.* **2018**, *17*, 372–376. [CrossRef] [PubMed]
95. Saliba, M.; Matsui, T.; Domanski, K.; Seo, J.-Y.; Ummadisingu, A.; Zakeeruddin, S.M.; Correa-Baena, J.-P.; Tress, W.R.; Abate, A.; Hagfeldt, A.; et al. Incorporation of Rubidium Cations into Perovskite Solar Cells Improves Photovoltaic Performance. *Science* **2016**, *354*, 206–209. [CrossRef] [PubMed]
96. Rong, Y.; Hu, Y.; Mei, A.; Tan, H.; Saidaminov, M.I.; Seok, S.I.; McGehee, M.D.; Sargent, E.H.; Han, H. Challenges for Commercializing Perovskite Solar Cells. *Science* **2018**, *361*, eaat8235. [CrossRef] [PubMed]
97. Torrence, C.E.; Libby, C.S.; Nie, W.; Stein, J.S. Environmental and Health Risks of Perovskite Solar Modules: Case for Better Test Standards and Risk Mitigation Solutions. *iScience* **2023**, *26*, 105807. [CrossRef] [PubMed]
98. *IEC 61215-1:2021*; Terrestrial Photovoltaic (PV) Modules–Design Qualification and Type Approval–Part 1: Test Requirements. International Electrotechnical Commission (IEC): Geneva, Switzerland, 2021.
99. Aristidou, N.; Eames, C.; Sanchez-Molina, I.; Bu, X.; Kosco, J.; Islam, M.S.; Haque, S.A. Fast Oxygen Diffusion and Iodide Defects Mediate Oxygen-Induced Degradation of Perovskite Solar Cells. *Nat. Commun.* **2017**, *8*, 15218. [CrossRef] [PubMed]
100. Zhou, H.; Chen, Q.; Li, G.; Luo, S.; Song, T.; Duan, H.-S.; Hong, Z.; You, J.; Liu, Y.; Yang, Y. Interface Engineering of Highly Efficient Perovskite Solar Cells. *Science* **2014**, *345*, 542–546. [CrossRef] [PubMed]
101. Mei, A.; Sheng, Y.; Ming, Y.; Hu, Y.; Rong, Y.; Zhang, W.; Luo, S.; Na, G.; Tian, C.; Hou, X.; et al. Stabilizing Perovskite Solar Cells to IEC61215:2016 Standards with over 9,000-h Operational Tracking. *Joule* **2020**, *4*, 2646–2660. [CrossRef]
102. Zhang, D.; Li, D.; Hu, Y.; Mei, A.; Han, H. Degradation Pathways in Perovskite Solar Cells and How to Meet International Standards. *Commun. Mater.* **2022**, *3*, 58. [CrossRef]
103. Bhati, N.; Dyson, P.J.; Nazeeruddin, M.K.; Maréchal, F. Techno-Economic Analysis Framework for Perovskite Solar Module Production at Various Manufacturing Capacities. *Renew. Energy* **2026**, *256*, 123752. [CrossRef]
104. Song, Z.; McElvany, C.L.; Phillips, A.B.; Celik, I.; Krantz, P.W.; Watthage, S.C.; Liyanage, G.K.; Apul, D.; Heben, M.J. A Technoeconomic Analysis of Perovskite Solar Module Manufacturing with Low-Cost Materials and Techniques. *Energy Environ. Sci.* **2017**, *10*, 1297–1305. [CrossRef]
105. Moody, N.; Sesena, S.; deQuilettes, D.W.; Dou, B.D.; Swartwout, R.; Buchman, J.T.; Johnson, A.; Eze, U.; Brenes, R.; Johnston, M.; et al. Assessing the Regulatory Requirements of Lead-Based Perovskite Photovoltaics. *Joule* **2020**, *4*, 970–974. [CrossRef]
106. *IEC 61730-1:2023*; Photovoltaic (PV) Module Safety Qualification–Part 1: Requirements for Construction. International Electrotechnical Commission (IEC): Geneva, Switzerland, 2023.
107. Holzhey, P.; Prettl, M.; Collavini, S.; Chang, N.L.; Saliba, M. Toward Commercialization with Lightweight, Flexible Perovskite Solar Cells for Residential Photovoltaics. *Joule* **2023**, *7*, 257–271. [CrossRef]
108. Zhu, H.; Teale, S.; Lintangpradipto, M.N.; Mahesh, S.; Chen, B.; McGehee, M.D.; Sargent, E.H.; Bakr, O.M. Long-Term Operating Stability in Perovskite Photovoltaics. *Nat. Rev. Mater.* **2023**, *8*, 569–586. [CrossRef]
109. McGovern, L.; Garnett, E.C.; Veenstra, S.; Van Der Zwaan, B. A Techno-Economic Perspective on Rigid and Flexible Perovskite Solar Modules. *Sustain. Energy Fuels* **2023**, *7*, 5259–5270. [CrossRef] [PubMed]
110. Huang, J.; Yuan, Y.; Shao, Y.; Yan, Y. Understanding the Physical Properties of Hybrid Perovskites for Photovoltaic Applications. *Nat. Rev. Mater.* **2017**, *2*, 17042. [CrossRef]
111. Kasar, A.K.; Menezes, P.L. Surface Engineering of Solar Cells to Improve Efficiency. *JOM* **2019**, *71*, 4319–4329. [CrossRef]
112. Christians, J.A.; Miranda Herrera, P.A.; Kamat, P.V. Transformation of the Excited State and Photovoltaic Efficiency of $CH_3NH_3PbI_3$ Perovskite upon Controlled Exposure to Humidified Air. *J. Am. Chem. Soc.* **2015**, *137*, 1530–1538. [CrossRef] [PubMed]
113. Park, N.-G. Perovskite Solar Cells: An Emerging Photovoltaic Technology. *Mater. Today* **2015**, *18*, 65–72. [CrossRef]
114. Bella, F.; Griffini, G.; Correa-Baena, J.-P.; Saracco, G.; Grätzel, M.; Hagfeldt, A.; Turri, S.; Gerbaldi, C. Improving Efficiency and Stability of Perovskite Solar Cells with Photocurable Fluoropolymers. *Science* **2016**, *354*, 203–206. [CrossRef] [PubMed]

Disclaimer/Publisher's Note: The statements, opinions and data contained in all publications are solely those of the individual author(s) and contributor(s) and not of MDPI and/or the editor(s). MDPI and/or the editor(s) disclaim responsibility for any injury to people or property resulting from any ideas, methods, instructions or products referred to in the content.